Elsevier Editorial System(tm) for Geomorphology
Manuscript Draft

Manuscript Number: GEOMOR-4376R2

Title: Tracking geomorphic signatures of watershed suburbanization with multitemporal LiDAR

Article Type: Research Paper

Keywords: LiDAR time series; urbanization; land cover change; digital elevation models; anthropogenic geomorphology; watershed

Corresponding Author: Mr. Daniel Kyle Jones, M.S.

Corresponding Author's Institution: U.S. Geological Survey

First Author: Daniel Kyle Jones, M.S.

Order of Authors: Daniel Kyle Jones, M.S.; Matthew E Baker, Ph.D; Andrew J Miller, Ph.D; S. Taylor Jarnagin, Ph.D; Dianna M Hogan, Ph.D

Abstract: Urban development practices redistribute surface materials through filling, grading, and terracing, causing drastic changes to the geomorphic organization of the landscape. Many studies document the hydrologic, biologic, or geomorphic consequences of urbanization using space-for-time comparisons of disparate urban and rural landscapes. However, no previous studies have documented geomorphic changes from development using multiple dates of high-resolution topographic data at the watershed scale. This study utilized a time series of five sequential Light Detection and Ranging (LiDAR) derived digital elevation models (DEMs) to track watershed geomorphic changes within two watersheds throughout development (2002-2008) and across multiple spatial scales (0.01-1 km2). Development-induced changes were compared against an undeveloped forested watershed during the same time period. Changes in elevations, slopes, hypsometry, and surface flow pathways were tracked throughout the development process to assess watershed geomorphic alterations. Results suggest that development produced an increase in sharp topographic breaks between relatively flat surfaces and steep slopes, replacing smoothly varying hillslopes and leading to greater variation in slopes. Examinations of flowpath distributions highlight systematic modifications that favor rapid convergence in unchanneled upland areas. Evidence of channel additions in the form of engineered surface conduits is apparent in comparisons of pre- and post-development stream maps. These results suggest that topographic modification, in addition to impervious surfaces, contributes to altered hydrologic dynamics observed in urban systems. This work highlights important considerations for the use of repeat LiDAR flights in analyzing watershed change through time. Novel methods introduced here may allow improved understanding and targeted mitigation of the processes driving geomorphic changes during development and help guide future research directions for development-based watershed studies.

GEOMORPHOLOGY JOURNAL EDITORIAL REVIEW

All editorial changes and suggestions were accepted and can be seen in the "LiDAR timeseries paper Final 032714 track changes.docx" document.

Highlights (for review)

- Sequential LiDAR DEMs used to track geomorphic changes during urbanization process
- Developing watersheds compared against undeveloped forested reference watershed
- Smoothly varying hillslopes replaced by sharp topographic breaks
- Evidence of channel burial coupled with additions of engineered runoff conduits
- Increased watershed connectivity independent of impervious surface cover and pipes

Tracking geomorphic signatures of watershed suburbanization with multitemporal LiDAR

Daniel K. Jones[a,b *], Matthew E. Baker[b,1], Andrew J. Miller[b,2], S. Taylor Jarnagin[c,3], Dianna M. Hogan[a,4]

[a]U.S. Geological Survey, Eastern Geographic Science Center, 12201 Sunrise Valley Drive, Reston, VA 20192, USA

[b]Department of Geography and Environmental Systems, University of Maryland, Baltimore County, Sondheim Hall, 1000 Hilltop Circle, Baltimore, MD 21250, USA

[c]U.S. Environmental Protection Agency (USEPA) Landscape Ecology Branch, Environmental Sciences Division, USEPA/ORD National Exposure Research Laboratory, Mail Drop E243-05 109 T.W. Alexander Drive, Research Triangle Park, NC 27711, USA

*Corresponding author. Present address: U.S. Geological Survey, Eastern Geographic Science Center, 12201 Sunrise Valley Drive, Reston, VA 20192, USA; Tel.: +1 (703) 648-5120; Fax: +1 (703) 648-4603; E-mail: dkjones@usgs.gov.

[1]E-mail: mbaker@umbc.edu.
[2]E-mail: miller@umbc.edu.
[3]E-mail: jarnagin.taylor@epa.gov.
[4]E-mail: dhogan@usgs.gov.

Abstract

Urban development practices redistribute surface materials through filling, grading, and terracing, causing drastic changes to the geomorphic organization of the landscape. Many studies document the hydrologic, biologic, or geomorphic consequences of urbanization using space-for-time comparisons of disparate urban and rural landscapes. However, no previous studies have documented geomorphic changes from development using multiple dates of high-resolution topographic data at the watershed scale. This study utilized a time series of five sequential Light Detection and Ranging (LiDAR) derived digital elevation models (DEMs) to track watershed geomorphic changes within two watersheds throughout development (2002-2008) and across multiple spatial scales (0.01-1 km^2). Development-induced changes were compared against an undeveloped forested watershed during the same time period. Changes in elevations, slopes, hypsometry, and surface flow pathways were tracked throughout the development process to assess watershed geomorphic alterations. Results suggest that development produced an increase in sharp topographic breaks between relatively flat surfaces and steep slopes, replacing smoothly varying hillslopes and leading to greater variation in slopes. Examinations of flowpath distributions highlight systematic modifications that favor rapid convergence in unchanneled upland areas. Evidence of channel additions in the form of engineered surface conduits is apparent in comparisons of pre- and post-development stream maps. These results suggest that topographic modification, in addition to impervious surfaces, contributes to altered hydrologic dynamics observed in urban systems. This work highlights important considerations for the use of repeat LiDAR flights in analyzing watershed change through time. Novel methods introduced here may allow improved understanding and targeted mitigation of the processes driving

geomorphic changes during development and help guide future research directions for development-based watershed studies.

Keywords: LiDAR time series; urbanization; land cover change; digital elevation models; anthropogenic geomorphology; watershed

1. Introduction

At least one-third of the Earth's continental surface has undergone some form of anthropogenic geomorphological activity (Rózsa, 2010). Of these activities, construction and urban development stand out as ongoing and expanding causes of geomorphic change characterized by rapid, complex, and multiscalar processes. Throughout urban development, extensive landscape grading, leveling, and terracing can change the fundamental organization of topography within a watershed (Tenenbaum et al., 2006; Csima, 2010). The current ability to track, quantify, and predict development-induced geomorphic changes is hindered by insufficient data and reliance on methodologies developed for traditional geomorphic studies in natural settings (Djokic and Maidment, 1991; Haff, 2003; Gironás et al., 2010; Rózsa, 2010; Szabo, 2010). High-resolution topographic data, such as Light Detection and Ranging (LiDAR), is required to resolve surface flowpaths and visualize roads and other fine-scale features in urban landscapes (Djokic and Maidment, 1991; Tenenbaum et al., 2006; Hunter et al., 2008; Gironás et al., 2010). Sequential topographic data sets are needed to track and quantify the multiscalar (Bochis and Pitt, 2005; Tenenbaum et al., 2006; Bochis, 2007) and temporally variable (MDE, 2000; Dietz and Clausen, 2008) topographic changes throughout development. No studies have utilized a high-resolution digital elevation model (DEM) time series to track geomorphic changes throughout the development process.

The topographic footprint of development is visually striking on the ground and from the air, highlighting large-scale landscaping carried out during initial development phases (Csima, 2010). Final smoothing and regrading occurs at finer scales that are less immediately apparent in topographic data, but are nonetheless important for understanding surficial drainage and altered geomorphic characteristics (MDE, 2000; Tenenbaum et al., 2006). How best to quantify such topographic changes is unclear in terms of selecting geomorphic variables and spatial scales that most effectively capture observed changes (Haff, 2003; Rózsa, 2010). Topographic variables such as slope, curvature, and their distribution relative to watershed area play important roles in sediment transport and erosion dynamics (Moore et al., 1991; Montgomery and Foufoula-Georgiou, 1993; James et al., 2007), channel formation (Band, 1993; Montgomery and Foufoula-Georgiou, 1993), and surface water – groundwater exchanges (Beven and Kirkby, 1979; Moore et al., 1991; Tenenbaum et al., 2006). However, topographic controls on hydrologic and geomorphic processes may be altered in urban landscapes because of infrastructure (e.g., roads, pipes) (Djokic and Maidment, 1991; Tenenbaum et al., 2006; Gironás et al., 2009; Rózsa, 2010; Choi, 2012).

Five sequential LiDAR-derived DEMs spanning the development of two small, historically agricultural watersheds were obtained to track geomorphic changes throughout development. The goal of this study is to understand how and where geomorphic changes manifest within these watersheds and to understand their implications for watershed geomorphic and hydrologic processes prior to accounting for influences of stormwater infrastructure. The DEM coverage of a third, forested reference watershed was used to track temporal variation not attributable to development. This work will introduce a number of novel methods for tracking temporal geomorphic changes using sequential LiDAR DEMs and will highlight unique geomorphic signatures of the development process. Results of this study will help guide ongoing research efforts that focus on the coupled influence of topography and infrastructure on watershed function.

2. Site description

For this study, three watersheds in Montgomery County, Maryland, within the Piedmont Physiographic Province were examined. All three watersheds are within the Mt. Airy Uplands District, characterized by siltstones and quartzite with underlying crystalline bedrock consisting of a phyllite/slate unit, with average annual precipitation of 106.4 cm (Reger and Cleaves, 2008; Hogan et al., ~~2013~~2014). Soper Branch (forested control) drains an area of ~ 3.4 km^2 with an overall mean gradient of 13%. Land cover is predominantly classified as deciduous forest (~ 85%) and small percentages of low-density housing and agriculture (6 and 9%, respectively) (Hogan et al., ~~2013~~2014; Dr. J.V. Loperfido, USGS, oral communication, July 2013). Tributaries 104 and 109 (T104 and T109, urbanizing) drain areas of ~ 1.2 and 0.9 km^2 with mean gradients of 11 and 8%, respectively. Tributaries 104 and 109 are historically agricultural watersheds that underwent extensive suburban development from 2003 to the present. Tributary 104 land use shifted from 41% agriculture, 0.3% barren, 42% forest, and 17% urban in 2002 to 2% agriculture, 15% barren, 19% forest, and 64% urban in 2008. Across the same time period, T109 changed from 64% agriculture, 1% barren, 25% forest, and 10% urban to 45% agriculture, 13% barren, 25% forest, and 17% urban (Hogan et al., ~~2013~~2014). Both T104 and T109 were used in analyses of development-induced geomorphic changes. However, development in T109 was not complete at the time of the last LiDAR flight, so the final T109 DEM represents a different stage of development than T104.

Tributaries 104 and 109 fall within the Clarksburg Special Protection Area (CSPA, established in 1994) and are subject to development guidelines and restrictions (Maryland DEP, 2013). Broadly speaking, the Special Protection Area designation identifies areas with high quality natural resources and requires ongoing and future development projects to implement best available water quality and quantity protection measures. Water quality and quantity measures often exceed minimum local and state regulations and include extensive Best Management Practices (BMPs) implementation during (sediment and erosion controls; S&EC) and after development (stormwater management; SWM) (Hogan et al., ~~2013~~2014). Each watershed has extensive storm sewer (SS) infrastructure in addition to noted BMP and SWM structures. While SS infrastructure likely plays a key role in dictating watershed hydrology, the purpose of this study is to document geomorphic changes and their hydrologic implications independent of SS influence. Ongoing research will incorporate SS infrastructure to distinguish its effects from geomorphic impacts and better account for watershed hydrologic dynamics.

3. Data description and methods

Five sequential LiDAR-derived 1-m bare-earth point clouds were collected at semiannual intervals from 2002 to 2008 to track development-induced topographic changes in T104 and T109 and background topographic changes in Soper Branch. Detailed LiDAR vendor, instrumentation, and accuracy information are provided by Jarnagin (2010). Building removal and bare-earth point cloud filtering was performed by each LiDAR vendor utilizing proprietary software, summarized in Table 1. Differences in bare-earth filtering algorithms used by different vendors may have caused interpolated topography within filtered building footprints to vary between dates. Therefore, topographic patterns within building footprints may reflect filtering artifacts and should be interpreted with a degree of uncertainty.

Insert Table 1 near here.

LiDAR was collected as part of a larger monitoring effort to track watershed changes throughout development and to document development effects on local resources through time (Jarnagin, 2008). Detailed comparisons between LiDAR spot elevations and field-surveyed elevations across a range of slope, elevation, and land use classes are reported by Gardina (2008) and Jarnagin (2010). One-meter resolution DEMs were interpolated from bare-earth point clouds using the natural neighbor interpolation algorithm (Sibson, 1981). The DEMs were then coarsened to 2-m horizontal resolution to smooth and reduce noise in the interpolated topography. All subsequent spatial analyses were performed using the interpolated 2-m DEMs in ArcMap 9.3[1] (~~Esri~~ESRI, Redlands, CA).

[1] Any use of trade, firm, or product names is for identification purposes only and does not imply endorsement by the U.S. Government.

3.1. Elevation change

Differencing sequential DEMs has been used to estimate sediment budgets, to identify nutrient and sediment sources and sinks (Thoma et al., 2005), and to track gully evolution through time (Perroy et al., 2010). Raw difference calculations, however, do not incorporate any estimate of the error inherent across different DEMs or LiDAR vendors (e.g., they imply that all observed elevation differences are real). Further, LiDAR precision has been shown to vary across land cover classes—with forest cover exhibiting the lowest precision (Gardina, 2008; Jarnagin, 2010). Therefore, comparisons of absolute elevation change estimates across differing land cover classes may be misleading.

To correct for the inherent variability in elevation estimates through time, DEM differences were expressed as standard deviations (SD) through time calculated for each pixel in each watershed as

$$SD = \sqrt{\frac{1}{N}\sum_{i=year}^{N}(x_i - \mu)^2} \quad (1)$$

where N is the number of DEM years (5), x_i is the elevation for a given pixel x in year i, and μ is the mean elevation of pixel x across the five DEM years. The distribution of elevation SDs in Soper Branch was then used to quantify background elevation variability in T104 and T109. The SD distribution in Soper Branch was filtered to exclude all known areas with recent anthropogenic activities or structures to assure the distribution of SDs were indicative of the background signal. Any remaining non-zero SD in Soper Branch was assumed to be attributable to either natural causes or uncertainty in the LiDAR data. Because of the decreased elevation precision observed within forested pixels (e.g., Gardina, 2008; Jarnagin, 2010), the use of Soper Branch to quantify background LiDAR variability was a conservative baseline for detecting change in nonforest areas. To detect elevation changes associated with the development process, resulting SD maps were classified based on the distribution of SDs in Soper Branch, with an additional class added to distinguish SD values outside of the range observed in Soper Branch. Classes represent SD values less than or equal to the mean, within three standard deviations of the mean, and SD values greater than three standard deviations from the mean. Any elevation change above the maximum SD observed in Soper Branch is assumed to be attributable to the development process.

3.2. Slope change

The distribution of local slopes from before and after development in T104 were quantified and classified to ranges relevant to landscape development decisions described by Csima (2010; Table 2). Each slope class in the pre-development landscape provides an indication of the relative development costs and earth-moving practices used across the watershed. A representative cross section was extracted for pre- (2002) and post- (2008) development years to highlight changes in the juxtaposition of high and low sloping areas and to differentiate spatial patterns associated with modified and unmodified areas. More broadly, changes in local terrain created by reallocating and relocating slopes were mapped using areal standard deviations of slope within a 10 x 10 pixel square neighborhood of every focal pixel x_i. Comparison of maps resulting from pre- and post-development DEMs further highlighted changes in the variability of local landscapes associated with development practices.

Insert Table 2 near here.

3.3. Hypsometric curves

Hypsometric curves represent the proportion of a watershed's area (*a/A*) that is above a given elevation (*h/H*), providing a generalized approximation of hillslope shape within the watershed. Traditionally, hypsometric curves have been used in discussions of landscape evolution across broad spatial extents (e.g., Strahler, 1957). Other studies have found hypsometric curve shape indicative of dominant erosional mechanisms (Harlin, 1980; Luo, 2000), hydrologic response (Luo and Harlin, 2003), and infiltration dynamics (Vivoni et al., 2008). Hypsometric curves were generated for each DEM year based on first-order catchment and full watershed scales to compare and contrast hillslope topographic alterations at increasingly broader spatial extents. Consistent boundaries were used for each year to assure that any hypsometric variability through time was attributable to topographic changes and not to boundary shifts caused by topographic modification along drainage divides. Hypsometric curves for each year were compared to assess hillslope level changes through time. A map of net fill and excavation (DEM_{2008} – DEM_{2002}) was also developed to help interpret hypsometric trends.

3.4. Drainage network change

Topographically based drainage network delineation methods are widely used across a range of land covers and climates. The most common approaches rely on threshold relationships of derivative watershed properties (e.g., drainage area, slope–~~—~~area relationship) to define upslope channel extents (e.g., O'Callaghan and Mark, 1984; Montgomery and Foufoula-Georgiou, 1993). Other techniques utilize local topography to extract convergent drainage features and stream heads directly (e.g., plan/profile curvature)~~,~~ but have seen much less use ~~due to~~because of higher topographic data resolution required for feature detection (Tribe, 1992; Band, 1993; Tarboton and Ames, 2001; Lindsay, 2006). A number of threshold-type approaches have been shown to provide reasonable approximations of field-surveyed channel networks (extent and complexity) (Heine et al., 2004; James et al., 2007; James and Hunt, 2010). However, threshold-based methods are insufficient for determining the location and occurrence of artificial urban conduits (e.g., swales, gutters) whose location is based on design specifications, not physical processes (Gironás et al., 2010; Jankowfsky et al., 2012).

Topographic openness (a measure of tangential curvature; see Yokoyama et al., 2002) was employed to identify surface networks in the pre-development terrain of T104 and then applied to the post-development terrain to compare surface network changes. Topographic openness is an angular relation of horizontal distance to vertical relief, calculated from above (positive/zenith) and below (negative/nadir) a topographic surface (DEM). For an angle ~~less than~~≤ 90°, openness is equivalent to the internal angle of an inverted cone, its apex at the focal DEM pixel, constrained by neighboring elevations within a specified radial distance. Topographic openness is more robust in identifying surface convexities and concavities than commonly used profile and plan curvature (Yokoyama et al., 2002) and has been successfully applied to LiDAR to identify convergent topography (Molloy and Stepinski, 2007; Sofia et al., 2011). Topographic openness was calculated using an Arc Macro Language (AML) script (written by M.E. Baker, UMBC ~~2005~~, personal communication, 2005) that reproduces the methods detailed in Yokoyama et al. (2002). The AML extracts DEM values for all relevant cells in a neighborhood set for each focal pixel x_i (defined by stepwise increments of one pixel width in each of eight azimuth directions until a specified search radius is reached; here we used 100 m) in a landscape. For each increment, the horizontal distance from and elevation above the focal pixel is calculated, and an arctan function converts opposite:adjacent ratios to angular degrees. The AML tracks a running maximum and minimum angle across each radial increment and all smaller increments for all eight directions, converts the resulting maxima and minima to zenith and nadir angles, and computes the mean of each across all eight directions. Thus the final openness values represent the averaged openness measure for all eight azimuths across the specified search radius.

Difference DEMs and ortho~~-~~imagery were used to identify detention basins and other potential barriers to surface flow. Pre- and post-development DEMs were filled to overcome internal drainages (i.e., ~~“~~‘pits~~”)~~ ‘) and then subtracted from unfilled DEMs to assess filling extents. Paths were carved from detention basin low points to the next downslope pixel of equal or lesser elevation outside of the filled zone. Where possible, carved pathways followed detention basin outlets identified from areal and ground surveys. No attempt was made to account for flowpaths within internal drainage basins or subsurface drainage infrastructure. Straight-line pathways were enforced for all unknown detention basin outlets. Flow directions were calculated for each year from the pit-resolved DEMs by enforcing drainage from each DEM pixel to the adjacent or diagonal pixel with the greatest drop in relief (see O'Callaghan and Mark, 1984).~~D8 flow directions were calculated for each year using the pit-resolved DEMs (e.g., O'Callaghan and Mark, 1984),~~ Resulting flow direction surfaces were used to generate drainage networks and other derivative surfaces~~from which drainage networks and other derivative surfaces were generated~~.

To create a stream map, ortho~~-~~imagery and hillshaded DEMs were overlain with openness grids to determine the critical openness for identifying surface depressions in the pre-development T104 DEM. A negative openness (nadir) angle of 91.5° ~~degrees~~ was determined to sufficiently capture all visible surface depressions. All pixels at or above 91.5° ~~degrees~~ were identified, and then connected using a D8-based accumulation operation to enforce downslope continuity from each depression (Tarboton and Baker, 2008). The pre-development stream map (as defined by downslope accumulation of depression pixels) was then tested for agreement with the constant drop law, which states that the mean elevation drop across channels within a given Strahler order should not be significantly different from the mean drop in the next higher order (Tarboton et al., 1991). Incremental accumulation thresholds of depression pixels were used to prune the pre-development stream map until it satisfied the constant drop law. The pre-development accumulation threshold was then applied to the post-development depression accumulation map to define the post-development stream map. Pre- and post-development stream maps were overlain and compared to assess network changes. Field visits were also conducted to classify channels as either natural (defined banks, sorted bed~~-~~load, evidence of ongoing or recent flow) or artificial (e.g., swales, outflow pipes, rip rap).

4. Results

Hillshades of each DEM year highlight the spatial pattern of surface modifications incrementally throughout development (~~Figure~~ Fig. 1). Initial large-scale resurfacing throughout the watershed is clear in 2004 and 2006 hillshades, with urban or suburban infrastructure distinguishable in the terrain. Fine-scale grading and smoothing that is much less visually apparent in the LiDAR characterize late-stage development in 2006 and 2008. Valley burial is evident in the western portion of the watershed (see red arrow in ~~Figure~~ Fig. 1), replaced by a smooth upland housing cluster and roadway. Mainstem valley form remained relatively constant throughout the time series, with little to no visual evidence of lateral channel movement.

Insert Figure 1 near here.

4.1. Elevation standard deviations

Pixelate elevation standard deviations (SD) calculated across the five DEM years were approximately normally distributed in Soper Branch with a mean of 0.063 m and a standard deviation of 0.034 m, ranging from 0.002~~-~~ to 0.870 m. Areas with temporal SDs greater than or equal to three standard deviations of the watershed mean (≥ 0.163 m) were focused within riparian zones at or near stream banks and near the basin outlet within a relatively flat and wide floodplain area (~~Figure~~ Fig. 2). Jarnagin (2010) reported similar LiDAR errors within densely vegetated riparian zones in comparisons between ground-truth and LiDAR spot elevations (absolute mean difference of 0.216 m with a standard deviation of 0.723 m and a maximum difference of 1.180 m). Moderately high SDs (0.063~~—~~–0.163 m) are also apparent on northeast- (NE) facing hillslopes. The temporal variation observed on ~~NE~~ NE-facing slopes was greater than systematic errors reported for ground survey and LiDAR-derived elevations, which exhibited a mean absolute difference of ~ 0.05 m (Gardina, 2008).

Elevation changes in T104 and T109 classified to the distribution of temporal SDs in Soper Branch highlight large areas exhibiting substantial elevation changes greater than the variability observed in forested controls. White areas in T104 and T109 signify temporal elevation SD values that are above the maximum observed in Soper Branch (> 0.870 m), encompassing ~~approximately~~ ~ 24.4% and 9.9% of total watershed area, respectively. Distinct patches of high elevation variability are primarily located in development parcels evident in the post-development hillshades (2008 panel in ~~Figure~~ Fig. 1). High temporal variability (0.163-0.870 m) is also apparent along the mainstem channel of T104~~,~~ but is less evident in T109. Relatively low temporal SD values in the southern undeveloped portion of T109 and within riparian zones in T104 reflect magnitudes of temporal variability similar to those observed in Soper Branch. Such heterogeneous distribution of elevation change is consistent with the observation that earth-moving practices were not spatially uniform across developing parcels.

Insert Figure 2 here.

4.2. Slopes

The footprint of development is clearly distinguishable from unmodified hillslopes in a visual comparison of pre- and post-development slope maps (~~Figure~~ Fig. 3). Development created abrupt slope changes in the landscape, replacing relatively smooth topographic profiles (i.e., gray boxes in inset). Moderate to high slope classes (> 12%) were present along roads, housing parcels, and stormwater management features, despite the use of bare-earth LiDAR with buildings removed by filtering. Valley infill is apparent in the slope transect between points *a* and *b* at ~ 180 m with no evidence of the original valley structure in the post-development topography. High-frequency variation between low slope and high slope features is evident in the slope transect between 420 and 580 m across a developed subdivision.

Formatted: Font: Italic

Formatted: Font: Italic

Insert Figure 3 here.

Areal slope standard deviations calculated using a 10 x 10 pixel moving window show a marked increase in the spatial variability of local slope values in post-development topography (~~Figure~~ Fig. 4). The overall distribution of variation in local slopes exhibited a positive shift from the pre- (mean areal slope standard deviation of 2.35 ± 2.26%) to post-development terrain (mean areal slope standard deviation of 4.69 ± 3.54%). Highly variable slope zones in 2002 were limited to riparian corridors and pre~~-~~existing development plots in the northern section of T104. By contrast, post-development slopes exhibit greater local variation (i.e., ~~both~~ steeper and flatter terrain in close proximity) associated with the grading of subdivisions and road embankments.

Insert Figure 4 here.

4.3. Hypsometry

Despite substantial topographic changes across the watershed visible in hillshades and slope maps representing different stages of development, hypsometric changes ~~due to~~owing to development only manifest when observed across small extents with relatively uniform, high magnitude surface changes (~~Figure~~ Fig. 5). Distinctly terraced hypsometric curves appear in the end-development phase topography, mirroring abrupt slope changes along roadways and surrounding housing parcels (see insets A and C in ~~Figure~~ Fig. 5). Valley infill in subwatershed A (see red arrow in ~~Figure~~ Fig. 1) created a sharp elevation gradient to the remaining riparian lowlands, reflected in the 2007 and 2008 hypsometric curves. Terracing and leveling of upslope transportation corridors also contribute to the terraced hypsometric form. Hypsometric trends of the larger subwatershed B~~,~~ and at the full watershed scale (D) did not exhibit detectable temporal changes.

Insert Figure 5 here.

4.4. Drainage network changes

Substantial redistribution of overland flowpaths is evident in comparisons of pre- and post-development flow direction grids (~~Figure~~ Fig. 6). As with slope comparisons, the most drastic changes in flow directions are focused along roadways and within housing parcels. Small patches of uniform flow directions mirroring housing and road footprints have replaced large, contiguous patches of homogenous flow directions (i.e., parallel flow lines) on upland hillslopes. Fine-scale variation in flow directions within relatively minor elevation change zones (see elevation change inset in ~~Figure~~ Fig. 6) are coupled with more dramatic modifications within drainage features and near infrastructure. As a result of these alterations to the flow field, flow accumulation distributions exhibited a negative shift, with accumulation quartiles decreasing from 4, 11, and 29 pixels in 2002 to 1, 4, and 12 pixels in 2008. Distributional shifts reflect drainage dissection and the fragmented flow field apparent in ~~Figure~~ Fig. 6 with small, locally convergent pathways replacing large, contiguous, parallel flowpaths.

Insert figure 6 here.

A depression pixel (openness ≥ 91.5º) accumulation threshold of three pixels was found to satisfy the constant drop criterion in the pre-development terrain of T104. The three-pixel threshold was then applied to the post-development terrain to evaluate surface network changes. Comparisons of pre- and post-development drainage network structure in T104 indicate a net gain in stream length of 4.25 km (~ 52% increase) throughout the watershed (~~Figure~~ Fig. 7). Additions were common along transportation infrastructure as swales or gutters typical in this watershed. Upslope extensions of existing channels also occurred extending beyond pre~~-~~existing piped infrastructure at the apparent head of pre-development drainage lines (~~inset A in Figure~~ Fig. 7A). Valley infill (~~see subwatershed A in Figure~~ see Fig. 6A) caused the loss of a tributary~~,~~ but was replaced by an artificial conduit that paralleled a nearby road (~~inset B in Figure~~ Fig. 7B). Similar conduits are apparent on the eastern side of the watershed as well (~~inset C in Figure~~ Fig. 7C). No substantial changes were apparent in the mainstem channel as suggested by the near 1:1 overlap in pre- and post-development networks.

Insert Figure 7 here.

5. Discussion

The growing footprint of development in T104 is clearly visible in the DEM hillshade time series, with distinct early- and late-stage development phases operating at unique spatial scales (~~Figure~~ Fig. 1). Large-scale cutting and filling to support major infrastructure characterizes early development, evident in the 2004 and 2006 hillshades. In contrast, fine-scale leveling and grading of housing parcels characterize late-stage development (MDE, 2000). Fine-scale ~~earth moving~~earth-moving practices are less immediately apparent in hillshades~~,~~ but are detectable in derivative data sets, as this study has shown. Results show that geomorphic changes associated with urban development are significant and non~~-~~uniform~~,~~ and could have implications for management and conservation efforts.

Initial analysis of background elevation changes in Soper Branch revealed non~~-~~zero standard deviations focused on northeast- (NE) facing hillslopes~~,~~ and within riparian and floodplain areas (~~Figure~~ Fig. 2). Increased variation on NE hillslopes may reflect flight paths taken during LiDAR collection~~,~~ or possible aspect differences in vegetation and soils. Slightly lower systematic errors reported in Gardina (2008) were attributed in part to methods used to derive bare-earth point clouds~~,~~ and, in part, to LiDAR system error. ~~It is likely that t~~The NE artifact likely is a combination of vegetation and LiDAR system errors. Riparian and floodplain variability in Soper Branch can be attributed to LiDAR errors reported by Jarnagin (2010). In comparisons between LiDAR elevations and ~~field ~~field-surveyed spot elevations, Jarnagin observed greater LiDAR error in densely vegetated riparian zones and on steep slopes common around incised channels. Distinguishing temporal variability attributable to artifacts in the LiDAR time series was necessary before reaching any quantitative conclusions about topographic changes resulting from development.

Elevation standard deviations classified to distinguish background and development-induced changes clearly show that earth moving in T104 and T109 was nonetheless substantially greater than background geomorphic changes observed in Soper Branch. Magnitudes similar to temporal standard deviations found in Soper Branch were observed in T104 across pre~~-~~existing housing parcels and riparian zones left untouched to comply with riparian protection policies. Somewhat higher variability observed along the mainstem channel in T104 may indicate subtle channel shifts and bank erosion throughout the time period despite attempts to insulate the channel from the hydrologic and geomorphic effects of development. ~~It is a~~Also, ~~possible that ~~some of the observed elevation changes may possibly reflect artifacts produced by removing buildings from the raw LiDAR point clouds. Because of the proprietary nature of the LiDAR processing, ~~it was not possible to ~~evaluating~~e~~ the bare-~~-~~earth detection algorithms used by the data providers was not possible for this study.

Surface changes throughout development in T104 and T109 altered slopes to support infrastructure, enforce drainage, and promote infiltration. Comparison of pre- and post-development slope maps in T104 shows a marked increase in high slope classes with development as well as reallocation across space (~~Figure ~~Fig. 3). High slope classes focused along transportation corridors and surrounding detention basins are likely to promote surface drainage. Slopes leading toward streams in the pre-development map appear to steepen with development as well, likely reflecting upland filling and terracing. Stream burial is a frequently cited phenomenon in urban watersheds (Leopold et al., 2005; Elmore and Kaushal, 2008; Roy et al., 2009; Doyle and Bernhardt, 2011) and is apparent on the western side of T104 (~ 180 m in transect inset of ~~Figure~~ Fig. 3). However, ~~it is unclear~~ without infrastructure design documents it is difficult to determine whether the stream is piped under its original flowpath~~,~~ or if it has been redirected to flow alongside the nearby ~~main~~ road running north to south.

Regular shifts between high and low slopes within subdivisions likely reflect housing parcels (low slopes) separated by graded lawns and swales (higher slopes) to promote drainage (~~Figure~~ Fig. 4). Low slopes within building footprints reflect the building removal algorithm applied to LiDAR point clouds to extract bare-earth points used in this study to create DEMs. The spatial distribution of high and low slopes in part controls the spatial distribution of runoff generation and infiltration zones (Beven and Kirkby, 1979; Tenenbaum et al., 2006). Shifts in the spatial pattern and magnitude of slopes may contribute to altered watershed processes including runoff generation, nutrient and sediment transport, and surface ~~water-groundwater~~ water – groundwater exchanges.

Hypsometric trends within small subwatersheds of T104 appear to mirror aforementioned steepening of valley walls with development (~~Figure~~ Fig. 5). Upland filling and grading further exacerbates the disparity in elevations between the ~~now~~ now-developed uplands and the riparian lowlands. Redistribution of flowpaths at and around valley infills likely altered surface and subsurface water exchanges, thus changing the functional connectivity of upland and lowland areas. Dynamics are further complicated by stormwater management infrastructure, such as detention ponds and infiltration trenches, typically located between upland (development plots) and lowland (riparian zone) areas to capture and treat overland runoff before it enters local streams (Montgomery County Planning Department, 1994). Thus, riparian areas may no longer be functionally connected to upland areas during rain events unless stormwater management outfalls are triggered. Further research is required to investigate the nature of the altered ~~surface-groundwater~~ surface – groundwater connections. Lack of temporal trends in the larger subwatershed topography or throughout the entire watershed result from spatial averaging~~,~~ and may indicate a detection limit for tracking parcel or block-level topographic change with hypsometry.

Development caused a substantial reconfiguration of overland flowpaths from large contiguous areas of uniform directions to small, spatially fragmented patches (~~Figure~~ Fig. 6). The non-random distribution of smaller patches mirrors housing footprints, transportation corridors, and stormwater management infrastructure~~,~~ and reflects landscape-engineering practices that promote efficient collection and drainage of overland runoff (~~Figure~~ Fig. 7). Adjacent pixels with uniform directions indicate parallel flowpaths, which will not converge until a pixel with a differing direction is encountered downslope (O'Callaghan and Mark, 1984). By introducing heterogeneity into the flow direction surface, development has created both more dissected subbasins and increased opportunities for small flowpaths to converge. Increased convergence in upland areas causes overland flow to reach moderately low accumulations more often and very high accumulations more rarely than in the pre-development terrain. Decreased median and ~~first~~

first-quartile values between 2002 and 2008 reflect the dominance of low accumulation pathways with development. Such alterations are likely the cumulative result of many site-specific efforts to increase local water conveyance, but their cumulative effect should also have implications for patterns of soil moisture, variable source area, erosion, infiltration, and recharge (Beven and Kirkby, 1979; Moore et al., 1991; Tenenbaum et al., 2006). To our knowledge, a geomorphic driver of increased upland convergence in developed terrain has yet to be described in the literature. Typically, pipes and impervious surfaces are thought to be the causal agents of altered runoff, nutrient, and sediment dynamics in urban watersheds (e.g., Paul and Meyer, 2001; Dietz and Clausen, 2008; Roy et al., 2008). However, our results indicate that the geomorphic modifications that occur with development are substantial and could also contribute to altered watershed functions.

Comparisons of pre- and post-development drainage networks reveal channel additions through engineered surface conduits (e.g., swales, culverts)~~,~~ and losses ~~due to~~caused by valley infill or subsurface routing (~~Figure~~ Fig. 7). Despite noted variability in elevations along stream banks, only minor shifts were apparent in the mainstem of T104. Results of this study also raise questions about what constitutes a channel in an urban landscape. Traditional channel definitions, characterized by defined banks and sorted bedloads (Montgomery and Dietrich, 1989; Heine et al., 2004) exclude engineered surface conduits that become active during precipitation events (Doyle and Bernhardt, 2011). Excluding these artificial conduits and subsurface stormwater pipes may under~~-~~represent the surficial connectivity of urban watersheds. Without infrastructure design documents, the true drainage connectivity of the watershed is unclear. Ongoing work will explore methods for incorporating subsurface drainage features into

T104 network representations (e.g., Gironás et al., 2009; Choi, 2012; Jankowfsky et al., 2012) and determine how best to incorporate BMP infrastructure into predicted network representations. Nevertheless, this study indicates an overall increase in surface connectivity with development independent of changes in impervious surface cover or subsurface stormwater infrastructure. Increased connectivity would result in faster and larger storm peaks if left unchecked by stormwater management infrastructure. Therefore, considering geomorphic changes in addition to impervious surface cover impacts is important for remediation efforts in urban areas.

6. Conclusions

This study has shown the utility of sequential LiDAR-derived DEMs for tracking and quantifying the geomorphic changes associated with development. Using a forested watershed as a reference, background topographic variability was quantified and differentiated from development-induced topographic change. Utilizing first- and second-order topographic derivatives, this study demonstrated that development generates increasingly disjointed hillslopes characterized by abrupt slope changes separating flat upland areas. Temporal variation in elevations, slopes, and hypsometric curves likely contributes to altered watershed functions, but further research is required to understand their importance relative to stormwater infrastructure. Substantial modification of overland flowpaths resulted in subtle changes to delineated network structure, highlighting additions and losses to the pre-development network. This study's ability to detect natural and manmade ephemeral surface conduits provides a more complete accounting of watershed hydrologic connectivity. Better accounting of upslope ephemeral channel extensions may help in designating areas for protection in future development projects. The geomorphic signal of increased landscape convergence and drainage density indicates more rapid runoff generation and conveyance independent of impervious surface cover or storm sewers. A better understanding of how and where geomorphic changes occur throughout development may enable a better understanding of pollutant mobilization and retention processes. Ongoing work seeks to incorporate known subsurface pipe and BMP structures into surface network representations to understand watershed hydrologic response dynamics.

Results presented here raise important considerations for temporal topographic studies. Standard topographic methods developed for use in larger, mostly non~~-~~urban watersheds (e.g., DEM differencing, hypsometry) have limited applicability for tracking urbanization unless summarized across a relatively small extent. Additional research is needed to gain a better understanding and to develop novel methods for tracking and quantifying urban topographic modifications.

~~7.~~ **Acknowledgements**

LiDAR funding provided in part by the U.S. Environmental Protection Agency under contract number EP-D-05-088 to Lockheed Martin. The U.S. Environmental Protection Agency through its Office of Research and Development collaborated in the research described here. This manuscript has been subjected to Agency review and approved for publication. This work would not have been possible without the Clarksburg Integrated Study Partnership, which includes the U.S. Environmental Protection Agency Landscape Ecology Branch (USEPA LEB), Montgomery County Department of Environmental Protection (DEP), the U.S. Geological Survey Eastern

Geographic Science Center (USGS EGSC), the University of Maryland (UMD), and the University of Maryland, Baltimore County (UMBC). We would like to thank Adam Bentham and one anonymous referee for providing constructive feedback on our paper during the review process.

~~8.~~ References

Band, L.E., 1993. Extraction of c~~C~~hannel n~~N~~etworks and t~~T~~opographic p~~P~~arameters from d~~D~~igital e~~E~~levation d~~D~~ata. In: ~~K.J.~~ Beven, K.J., ~~and M.J.~~ Kirkby, M.J. (~~Editors~~Eds.), Channel Network Hydrology. Wiley, New York, NY, pp. 13-42.

Formatted: Line spacing: Double

Beven, K.J., ~~and~~ Kirkby, M.J., 1979. A physically based, variable contributing area model of basin hydrology. Hydrological Sciences Bulletin~~,~~ 24(1),~~:~~ 43-69.

Bochis, E.C., 2007. Magnitude of impervious surfaces in urban areas. M.S. Thesis, University of Alabama, Tuscaloosa, 165 pp.

Bochis, E.C., ~~and~~ Pitt, R., 2005. Site development characteristics for stormwater modeling~~,~~. In: 78th Annual Water Environment Federation Technical Exposition and Conference, Washington, D.C., October 29-November 2. Washington, D.C., ~~p~~p. 37.

Formatted: Line spacing: Double

~~Bochis, E.C., 2007. Magnitude of impervious surfaces in urban areas, University of Alabama, Tuscaloosa, 165 pp.~~

Choi, Y., 2012. A new algorithm to calculate weighted flow-accumulation from a DEM by considering surface and underground stormwater infrastructure. Environmental Modelling & Software~~,~~ 30(0~~):~~), 81-91.

Csima, P., 2010. Urban development and anthropogenic geomorphology. In: ~~J.~~ Szabó, J., ~~L.~~ Dávid, L.~~and~~ ,~~D.~~ Lóczy, D. (Ed~~itor~~s.), Anthropogenic Geomorphology: A Guide to Man-Made Landforms. Springer, New York, NY, pp. 179-187.

Dietz, M.E., ~~John C.~~ Clausen, J.C., 2008. Stormwater runoff and export changes with development in a traditional and low impact subdivision. Journal of Environmental Management~~,~~ 8,~~:~~ 7.

Formatted: Line spacing: Double

Djokic, D., ~~and~~ Maidment, D.R., 1991. Terrain analysis for urban stormwater modelling. Hydrological Processes~~,~~ 5(1~~):~~), 115-124.

Doyle, M.W., ~~and~~ Bernhardt, E.S., 2011. What is a stream? Environmental Science & Technology~~,~~ 45(2~~):~~), 354-359.

Elmore, A.J., ~~and~~ Kaushal, S.S., 2008. Disappearing headwaters: patterns of stream burial due to urbanization. Frontiers in Ecology and the Environment~~,~~ 6(6~~):~~), 308-312.

Gardina, V.J., 2008. Analysis of LIDAR data for fluvial geomorphic change detection at a small Maryland stream. ~~Master of Science of~~M.S. Thesis, Civil Engineering, University of Maryland, College Park, ~~College Park,~~ 156 pp.

Gironás, J., Niemann, J.D., Roesner, L.A., Rodriguez, F., ~~and~~ Andrieu, H., 2009. A morpho-climatic instantaneous unit hydrograph model for urban catchments based on the kinematic wave approximation. Journal of Hydrology~~,~~ 377~~:~~, 317-334.

Gironás, J., Niemann, J.D., Roesner, L.A., Rodriguez, F., ~~and~~ Andrieu, H., 2010. Evaluation of methods for representing urban terrain in stormwater modeling. Journal of Hydrologic Engineering 15(1),~~:~~ ~~14~~1-14.

Haff, P.K., 2003. Neogeomorphology, ~~prediction~~Prediction, and the Anthropic ~~landscape~~Landscape. American Geophysical Union, Washington, DC, ETATS-UNIS, 12 pp.

Harlin, J.M., 1980. The effect of precipitation variability on drainage basin morphometry. American Journal of Science~~,~~ 280(8~~):~~), 812-825.

Heine, R.A., Lant, C.L., ~~and~~ Sengupta, R.R., 2004. Development and comparison of approaches for automated mapping of stream channel networks. Annals of the Association of American Geographers~~,~~ 94(3~~):~~), 477-490.

Hogan, D.M., Jarnagin, S.T., Loperfido, J.V., ~~and~~ Van Ness, K., ~~2013~~2014. Mitigating the ~~Effects~~ effects of ~~Landscape~~ landscape ~~Development~~ development on ~~Streams~~ streams in ~~Urbanizing~~ urbanizing ~~Watersheds~~watersheds. Journal of the American Water Resources Association 50(1), 163-178.

Hunter, N.M., Bates, P.D., Neelz, S., Pender, G., Villanueva, I., Wright, N.G., Liang, D., Falconer, R.A., Lin, B., Waller, S., Crossley, A.J., ~~and~~ Mason, D.C., 2008. Benchmarking 2D hydraulic models for urban flooding. Proceedings of the ICE - Water Management~~,~~ 161(1~~):~~), 13-30.

James, L.A., Hunt, K.J., 2010. The LiDAR-side of headwater streams mapping channel networks with high-resolution topographic data. Southeastern Geographer 50(4), 523-539.

James, L.A., Watson, D.G., ~~and~~ Hansen, W.F., 2007. Using LiDAR data to map gullies and headwater streams under forest canopy: South Carolina, USA. Catena~~,~~ 71~~:~~ , 132-144.

~~James, L.A. and Hunt, K.J., 2010. The LiDAR-side of headwater streams mapping channel networks with high-resolution topographic data. Southeastern Geographer, 50(4): 523-539.~~

Jankowfsky, S., Branger, F., Braud, I., Gironás, J., ~~and~~ Rodriguez, F., 2012. Comparison of catchment and network delineation approaches in complex suburban environments: application to the Chaudanne catchment, France. Hydrological Processes~~.~~, doi: 10.1002/hyp.9506.

Jarnagin, S.T., 2008. Collaborative research: streamflow, urban riparian zones, BMPs, and impervious surfaces. U.S. Environmental Protection Agency, Washington, D.C., EPA/600/F-08/001.

Jarnagin, S.T., 2010. Using repeated LIDAR to characterize topographic changes in riparian areas and stream channel morphology in areas undergoing urban development: An accuracy assessment guide for local watershed managers. U.S. Environmental Protection Agency, Washington, D.C., EPA/600/R-10/120, p. 167.

Leopold, L.B., Huppman, R., ~~and~~ Miller, A.J., 2005. Geomorphic effects of urbanization in forty-one years of observation. Proceedings of the American Philosophical Society~~,~~ 149(3~~):~~), 349-371.

Lindsay, J.B., 2006. Sensitivity of channel mapping techniques to uncertainty in digital elevation data. International Journal of Geographical Information Science~~,~~ 20(6~~):~~), 669-692.

Luo, W., 2000. Quantifying groundwater-sapping landforms with a hypsometric technique. Journal of Geophysical Research: Planets~~,~~ 105(E1~~):~~), 1685-1694.

Luo, W., ~~and~~ Harlin, J.M., 2003. A theoretical travel time based on watershed hypsometry. Journal of the American Water Resources Association~~,~~ 39(4~~):~~), 785-792.

Maryland Department of the Environment (MDE), 2000. Maryland ~~stormwater~~ Stormwater ~~design~~ Design ~~manual~~Manual. Center for Watershed Protection and the Maryland Department of the Environment, Baltimore, MD.

~~(DEP),~~ Maryland Department of Environmental Protection (DEP), 2013. Special Protection Areas, http://www6.montgomerycountymd.gov/dectmpl.asp?url=/content/dep/water/whatarespas.asp.

Molloy, I., ~~and~~ Stepinski, T.F., 2007. Automatic mapping of valley networks on Mars. Computers & Geosciences~~,~~ 33(6~~):~~), 728-738.

Montgomery County Planning Department, 1994. Clarksburg Master Plan and Hyattstown Special Study Area. Montgomery County Planning Department, Silver Spring, MD.

Montgomery, D.R., ~~and~~ Dietrich, W.E., 1989. Source areas, drainage density, and channel initiation. Water Resources Research~~,~~ 25(8~~):~~), 1907-1918.

Montgomery, D.R., ~~and~~ Foufoula-Georgiou, E., 1993. Channel network source representation using Digital Elevation Models. Water Resources Research~~,~~ 29(12~~):~~), 3925-3934.

Moore, I.D., Grayson, R.B., ~~and~~ Ladson, A.R., 1991. Digital terrain modelling: A review of hydrological, geomorphological, and biological applications. Hydrological Processes~~,~~ 5(1~~):~~), 3-30.

O'Callaghan, J.F., ~~and~~ Mark, D.M., 1984. The extraction of drainage networks from digital elevation data. Computer Vision, Graphics, and Image Processing~~,~~ 28(3~~):~~), 323-344.

Paul, M.J., ~~and~~ Meyer, J.L., 2001. Streams in the urban landscape. Annual Review of Ecology and Systematics~~,~~ 32(1~~):~~), 333-365.

Perroy, R.L., Bookhagen, B., Asner, G.P., ~~and~~ Chadwick, O.A., 2010. Comparison of gully erosion estimates using airborne and ground-based LiDAR on Santa Cruz Island, California. Geomorphology~~,~~ 118~~:~~, 288-300.

Reger, J.P., ~~and~~ Cleaves, E.T., 2008. Draft physiographic map of Maryland and explanatory text for the physiographic map of Maryland. Maryland Geological Survey Open File Report 08-03-01.

Roy, A.H., Wenger, S.J., Fletcher, T.D., Walsh, C.J., Ladson, A.R., Shuster, W.D., Thurston, H.W., ~~and~~ Brown, R.R., 2008. Impediments and ~~Solutions~~ solutions to ~~Sustainable~~sustainable, ~~Watershed~~watershed-~~Scale~~ scale ~~Urban~~ urban ~~Stormwater~~ stormwater ~~Management~~management: ~~Lessons~~ lessons from Australia and the United States. Environmental Management~~,~~ 42~~:~~, 344-359.

Roy, A.H., Dybas, A.L., Fritz, K.M., ~~and~~ Lubbers, H.R., 2009. Urbanization affects the extent and hydrologic permanence of headwater streams in a midwestern US metropolitan area. Journal of the North American Benthological Society~~,~~ 28(4~~):~~), 911-928.

Rózsa, P., 2010. Nature and extent of human geomorphological impact: a review. In: Szabó, J., Dávid, L., Lóczy, D. (Eds.), Anthropogenic Geomorphology: A Guide to Man-Made Landforms. Springer, New York, NY, pp.~~In: J. Szabó, L. Dávid and D. Lóczy (Editors), Anthropogenic Geomorphology: A Guide to Man-Made Landforms. Springer, pp.~~ 273-290.

Sibson, R., 1981. A ~~Brief~~ brief ~~Description~~ description of ~~Natural~~ natural ~~Neighbour~~ neighbour ~~Interpolation~~interpolation. In: ~~V.~~ Barnett, V. (~~Editor~~Ed.), Interpreting Multivariate Data. John Wiley & Sons, New York, NY, pp. 21-36.

Sofia, G., Tarolli, P., Cazorzi, F., ~~and~~ Dalla Fontana, G., 2011. An objective approach for feature extraction: distribution analysis and statistical descriptors for scale choice and channel network identification. Hydrology and Earth System Sciences~~,~~ 15(5~~):~~), 1387-1402.

Strahler, A.N., 1957. Quantitative analysis of watershed geomorphology. Transactions of the American Geophysical Union~~,~~ 38~~:~~, 913-920.

Szabo, J., 2010. Anthropogenic geomorphology: Subject and system. In: Szabó, J., Dávid, L., Lóczy, D. (Eds.), Anthropogenic Geomorphology: A Guide to Man-Made Landforms. Springer, New York, NY, pp.~~In: J. Szabó, L. Dávid and D. Lóczy (Editors), Anthropogenic Geomorphology: A Guide to Man-Made Landforms. Springer, pp.~~ 3-10.

Tarboton, D.G., Ames, D.P., 2001. Advances in the Mapping of Flow Networks from Digital Elevation Data, The World Water and Environmental Resources Congress. ASCE, Orlando, Florida, May 20-24, pp. 166-175.

Tarboton, D.G., Baker, M.E., 2008. Towards an algebra for terrain-based flow analysis. In: Mount, N., Harvey, G., Aplin, P., Priestnall, G. (Eds.), Representing, Modeling and Visualizing the Natural Environment: Innovations in GIS 13. CRC Press, New York, NY, pp. 167-194.

Tarboton, D.G., Bras, R.L., ~~and~~ Rodriguez-Iturbe, I., 1991. On the extraction of channel networks from digital elevation data. Hydrological Processes~~,~~ 5(1~~):~~), 81-100.

~~Tarboton, D.G. and Ames, D.P., 2001. Advances in the Mapping of Flow Networks from Digital Elevation Data, The World Water and Environmental Resources Congress. ASCE, Orlando, Florida, USA, pp. 166-175.~~

~~Tarboton, D.G., and Baker, M.E., 2008. Towards an Algebra for Terrain-Based Flow Analysis. In: G.L.H. N. J. Mount, P. Aplin, and G. Priestnall (Editor), Representing, Modeling and Visualizing the Natural Environment: Innovations in GIS 13. CRC Press, pp. 167-194.~~

Tenenbaum, D.E., Band, L.E., Kenworthy, S.T., ~~and~~ Tague, C.L., 2006. Analysis of soil moisture patterns in forested and suburban catchments in Baltimore, Maryland, using

Formatted: Line spacing: Double

high-resolution photogrammetric and LIDAR digital elevation datasets. Hydrological Processes~~,~~ 20~~:~~, 219-240.

Thoma, D.P., Gupta, S.C., Bauer, M.E., ~~and~~ Kirchoff, C.E., 2005. Airborne laser scanning for riverbank erosion assessment. Remote Sensing of Environment~~,~~ 95(4~~):~~), 493-501.

Tribe, A., 1992. Automated recognition of valley lines and drainage networks from grid digital elevation models: a review and a new method. Journal of Hydrology~~,~~ 139~~:~~, 263-293.

Vivoni, E.R., Di Benedetto, F., Grimaldi, S., ~~and~~ Eltahir, E.A.B., 2008. Hypsometric control on surface and subsurface runoff. Water Resources Research~~,~~ 44(12~~):~~), W12502.

Yokoyama, R., Shirasawa, M., ~~and~~ Pike, R.J., 2002. Visualizing topography by openness: A new application of image processing to digital elevation models. Photogrammetric Engineering & Remote Sensing~~,~~ 68(3~~):~~), 257-265.

~~9.~~ List of Figures ~~and Tables~~

Fig. 1. Sequential light detection and ranging (LiDAR) derived digital elevation models (DEMs) spanning the development process in T104 show the topographic footprint of development increasing through time. Boxes highlight topographic differences between early- and late-stage development practices. The red arrow denotes a valley that was buried during development.

Fig. 2. Elevation change through time quantified as temporal standard deviations (SD) calculated for each DEM pixel. Map values are classified to the distribution of elevation variation observed in Soper Branch (forested control). Black and dark gray areas represent values below and within three standard deviations of the areal mean in Soper Branch, respectively. Light gray areas

represent temporal variation in elevation greater than three standard deviations above the areal mean in Soper Branch; whereas white areas are greater than the maximum, and both indicate areas of substantial development.

Fig. 3. Comparisons of pre- (2002) and post- (2008) development slope distributions in T104 classified to ranges relevant to development practices (see Table 2 after Csima, 2010). Inset shows a cross-sectional profile of slope along the dashed red line between points *a* and *c*. Substantial differences in the variability of local slopes are evident in the profile between developed (shaded zone) and undeveloped (unshaded) parcels. High slopes ring roads, swales, and detention features and manifest as high magnitude variation across the lateral transect.

Fig. 4. Areal slope standard deviations calculated using a 10x10 pixel moving window for pre- and post-development T104 slope maps. As in pixelate slope maps, highly variable slope zones are concentrated along road corridors and around detention ponds. Nevertheless, a substantial increase in the local variability of slope is apparent in 2008, with high standard deviation values widely distributed across the watershed.

Fig. 5. Hypsometric variability through time exhibits distinctly different patterns across first-order subwatersheds in T104 (A, B, and C). Hypsometry of relatively small subwatersheds that underwent substantial resurfacing (A ~ 0.09 km^2 and C ~ 0.03 km^2) shifted from smooth (black curves) to terraced curve forms (gray curves) reflecting grading of developed parcels. However, extensive resurfacing was not apparent in hypsometric trends of larger subwatersheds (B ~ 0.43 km^2) or at the full watershed scale (D ~ 1.18 km^2).

Fig. 6. Extensive topographic modification (e.g., C) associated with grading throughout development (2002-2008) causes substantial variation in overland flowpath directions and elevation change (D) in T104. Comparisons between pre- and post-development years show that fine-scale flow direction changes at the hillslope scale are coupled with the designed orientation and gradients of road networks (A and B, with each color representing a unique direction of overland flow). Large patches of a single color indicate parallel flow lines down a hillslope, whereas fragmentation of the 2002 map in 2008 necessarily indicates redirection and convergence of previously unconnected contributing areas.

Fig. 7. Comparison of pre- (blue lines) and post- (red dashed lines) development channel network delineations suggest increased network density with development in T104. Added channels include upslope extensions beyond existing culverts (A) and vegetated swales parallel to roadways (C). Comparisons to pre-development topography show a minor tributary that has been buried during development (B).

Table 1~~.~~
Building removal and bare-earth point cloud processing information for each LiDAR year provided by S.T. Jarnagin (~~2013,~~ personal communication, 2013).~~[1]~~[a]

LiDAR ~~Year~~year	Instrument	Vendor	Building ~~Removal~~ removal ~~Software~~software	Bare-earth ~~Filtering~~filtering
2002	Optech ALTM-2025	Airborne 1	Optech's REALM 2.27	Terrascan (running on Microstation)
2004	Optech ALTM-2033	Laser Mapping Specialists Inc.	Applanix POSPROC & Optech's REALM (versions not specified)	Spectra's Terramodel
2006	Optech ALTM-3100	Canaan Valley Institute	Optech's REALM (version not specified)	Microstation 8 with Terrascan
2007	Optech ALTM-3100	Canaan Valley Institute	Optech's REALM (version not specified)	Microstation 8 with Terrascan
2008	Leica ALS-50	Sanborn	Applanix POSPROC 4.3	Leica ALS post-processing and Terrasolid Terrascan

~~[1]Any~~ [a]Any use of trade, firm, or product names is for identification purposes only and does not imply endorsement by the U.S. Government.

Formatted: Space After: 0 pt, Line spacing: single

Formatted Table

Formatted: Left

Formatted: Left

Formatted: Left

Formatted: Left

Formatted: Left

Formatted: Left

Formatted: Space After: 0 pt, Line spacing: single

Table 2

Slope classes and associated economic costs and considerations for urban development (adapted from Csima, 2010)

Angle of slope	Development potential and the required landscaping
Up to 5%	Easy and economic development potential. In general, terracing not necessary; landscaping exclusively restricts to drainage. Relief does not pose a limit either to build-up density or building size.
5-12%	Increased development costs. Landscaping is inevitable; development is only possible with terracing and slope leveling. Somewhat limited development.
12-25%	Development potential at significant cost and labor expenditure, only with terraces and supporting walls provided. Major topographic transformation; relief fundamentally controls the type of development to be applied.
25-35%	Limited potential for urban development. Low building density with small-sized buildings.
Above 35%	Unsuitable for urban development.

Formatted Table

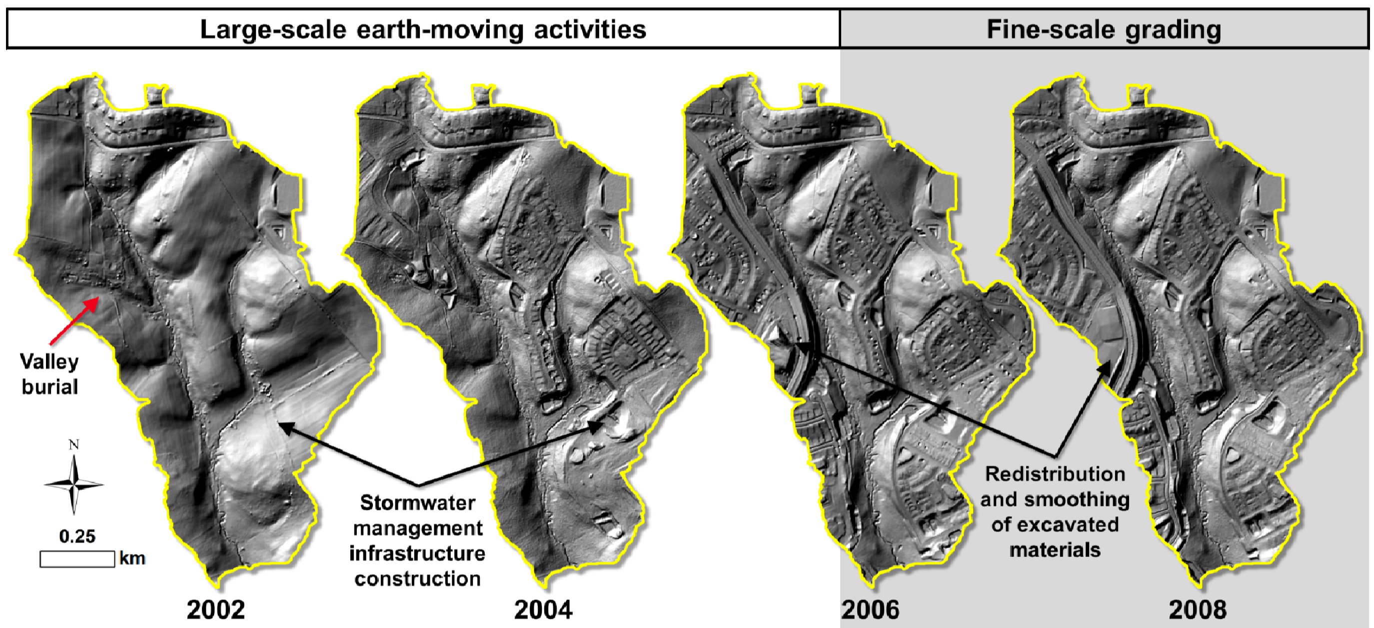

Large-scale earth-moving activities
Fine-scale grading
Valley burial
N
0.25
km
Stormwater management infrastructure construction
Redistribution and smoothing of excavated materials
2002
2004
2006
2008

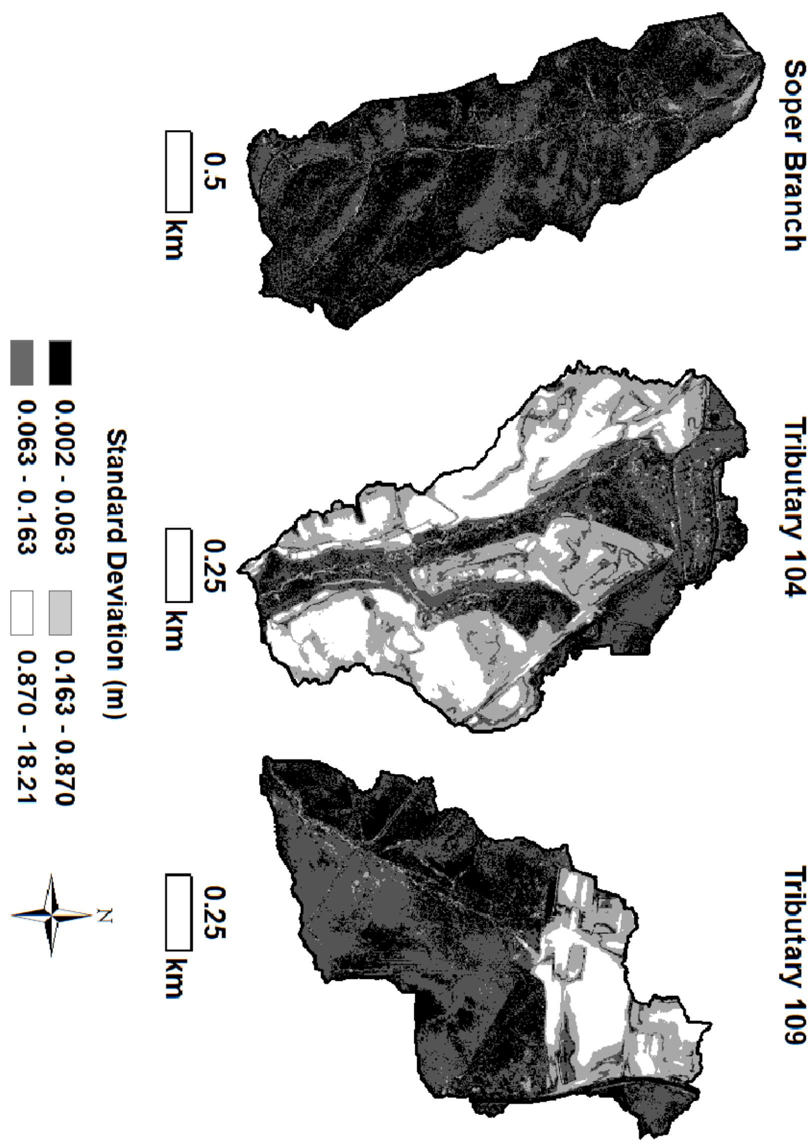
Soper Branch
Tributary 104
Tributary 109
0.5 km
0.25 km
0.25 km
Standard Deviation (m)
0.002 - 0.063
0.063 - 0.163
0.163 - 0.870
0.870 - 18.21
N

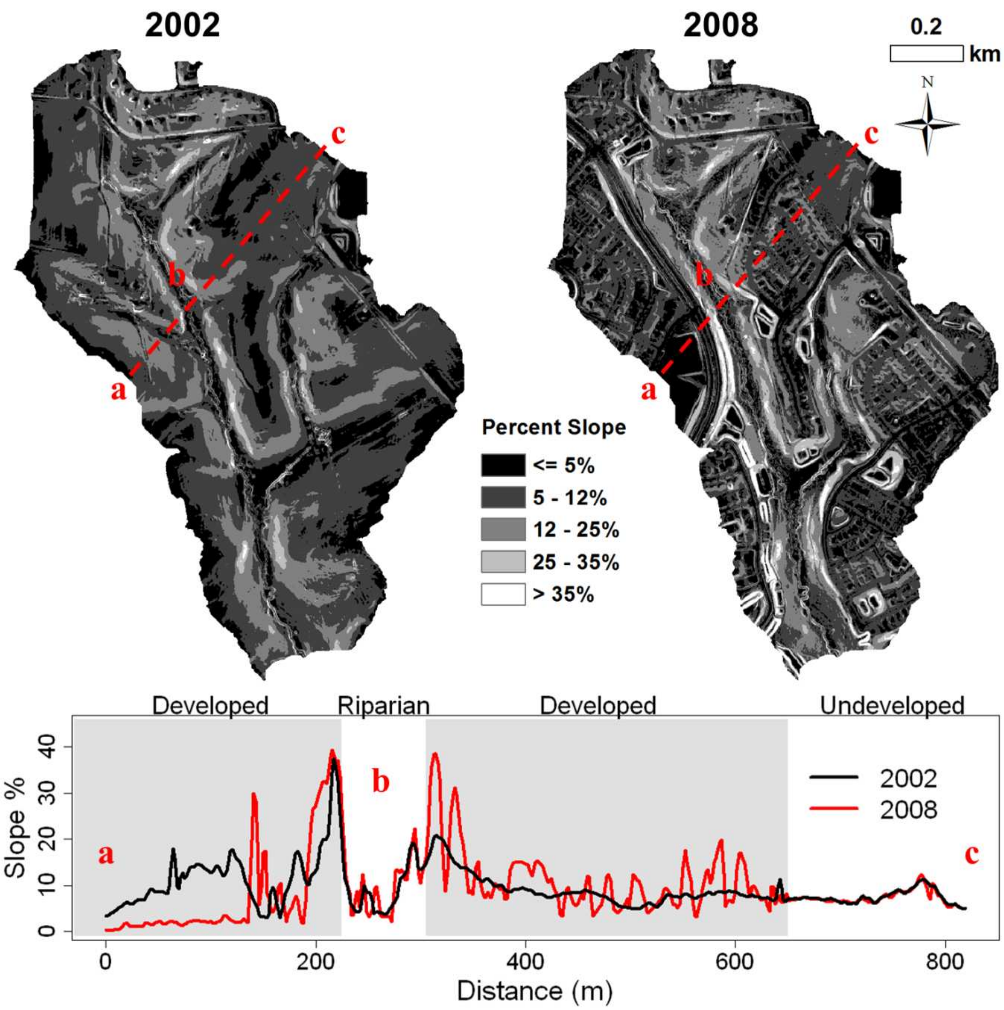
2002
2008
0.2
km
N
a
b
c
Percent Slope
<= 5%
5 - 12%
12 - 25%
25 - 35%
> 35%
Developed
Riparian
Developed
Undeveloped
Slope %
Distance (m)
2002
2008
0
10
20
30
40
200
400
600
800

795

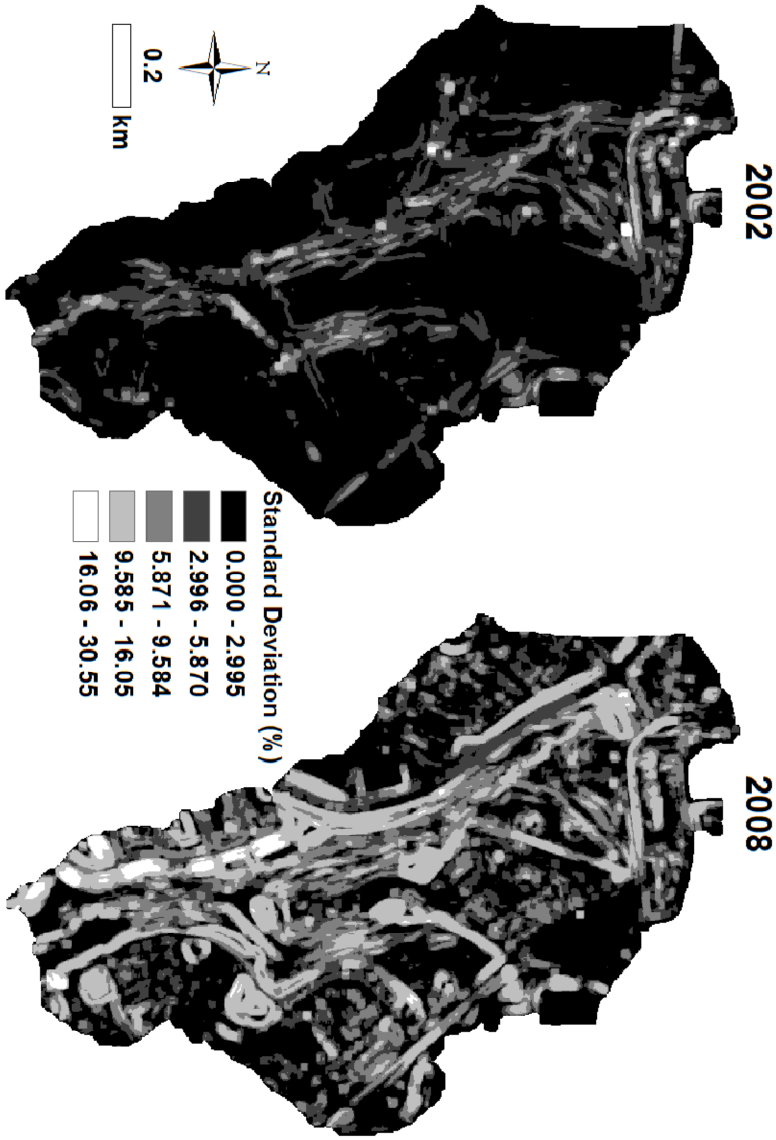
2002
2008
N
0.2
km
Standard Deviation (%)
0.000 - 2.995
2.996 - 5.870
5.871 - 9.584
9.585 - 16.05
16.06 - 30.55

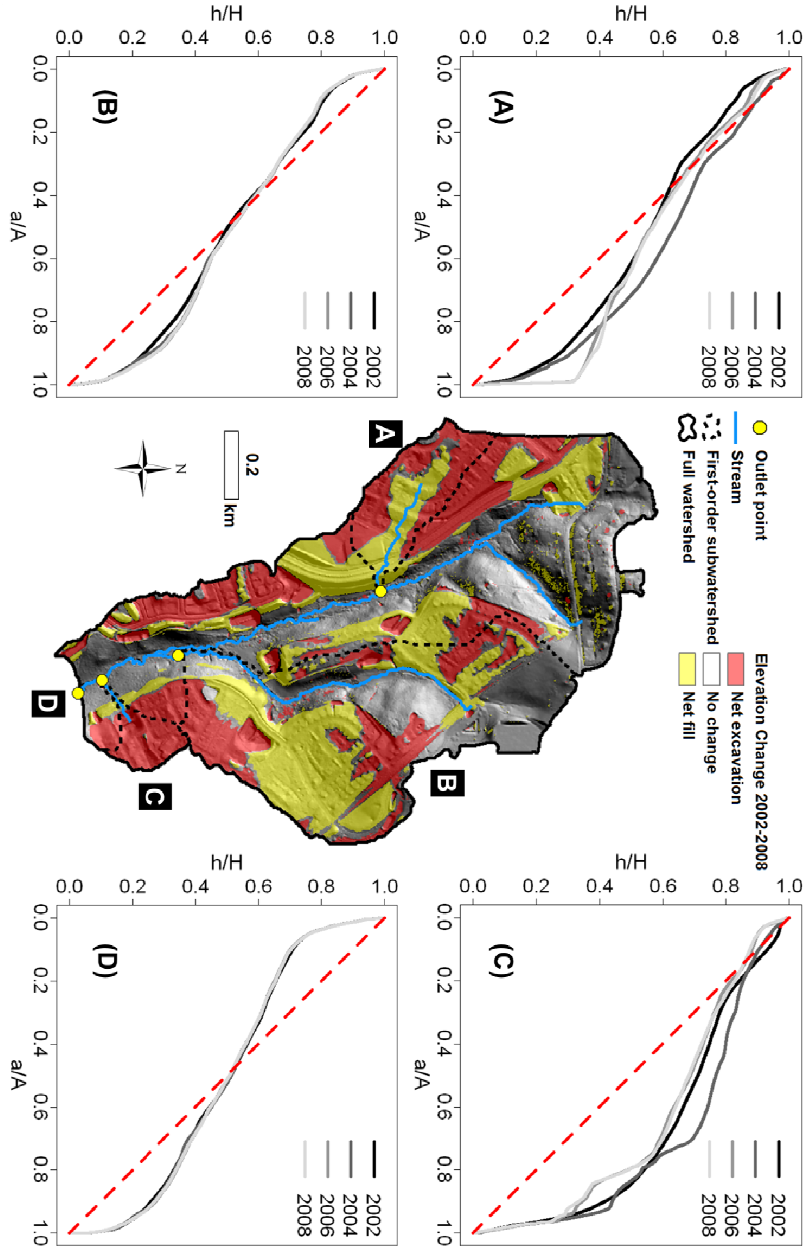
Outlet point
Stream
First-order subwatershed
Full watershed
Elevation Change 2002-2008
Net excavation
No change
Net fill
0.2
km
N
A
B
C
D
(A)
(B)
(C)
(D)
h/H
a/A
2002
2004
2006
2008

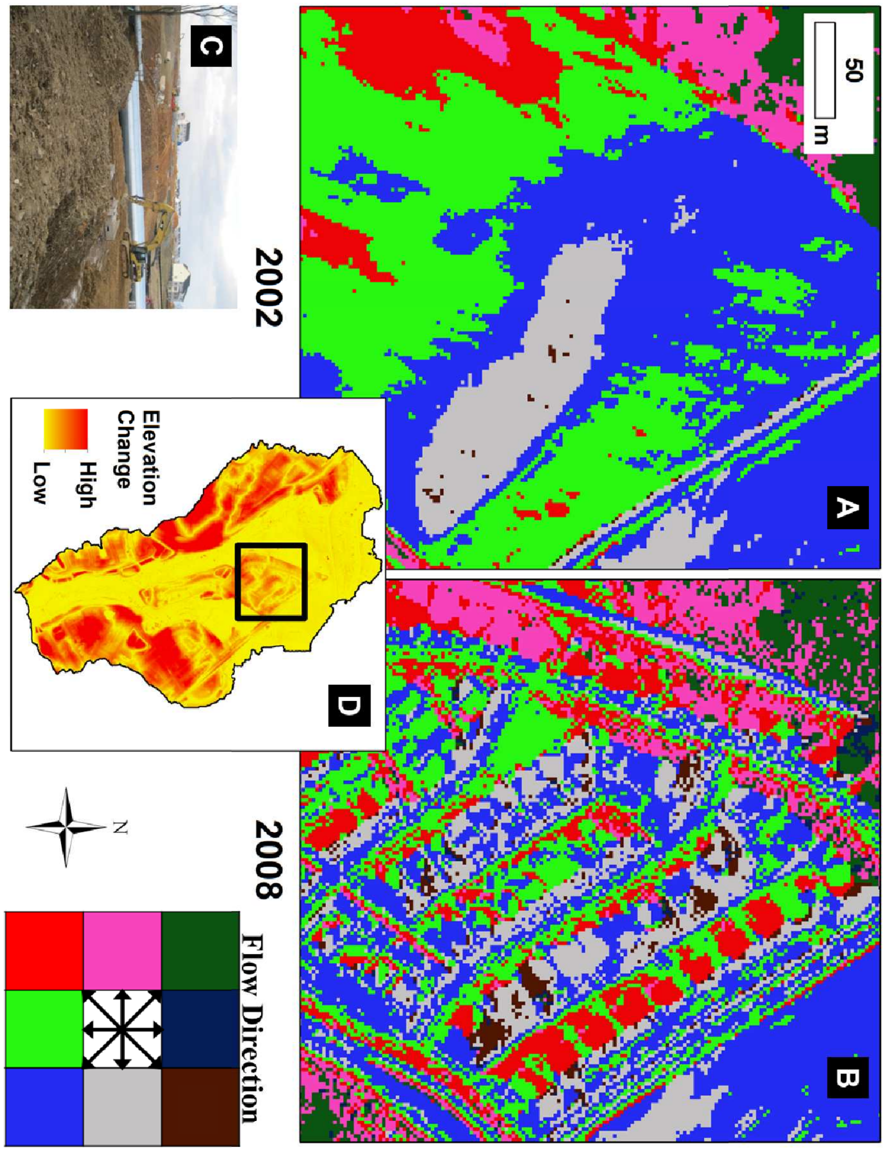
2002
2008
A
B
C
D
50 m
Elevation Change
High
Low
N
Flow Direction

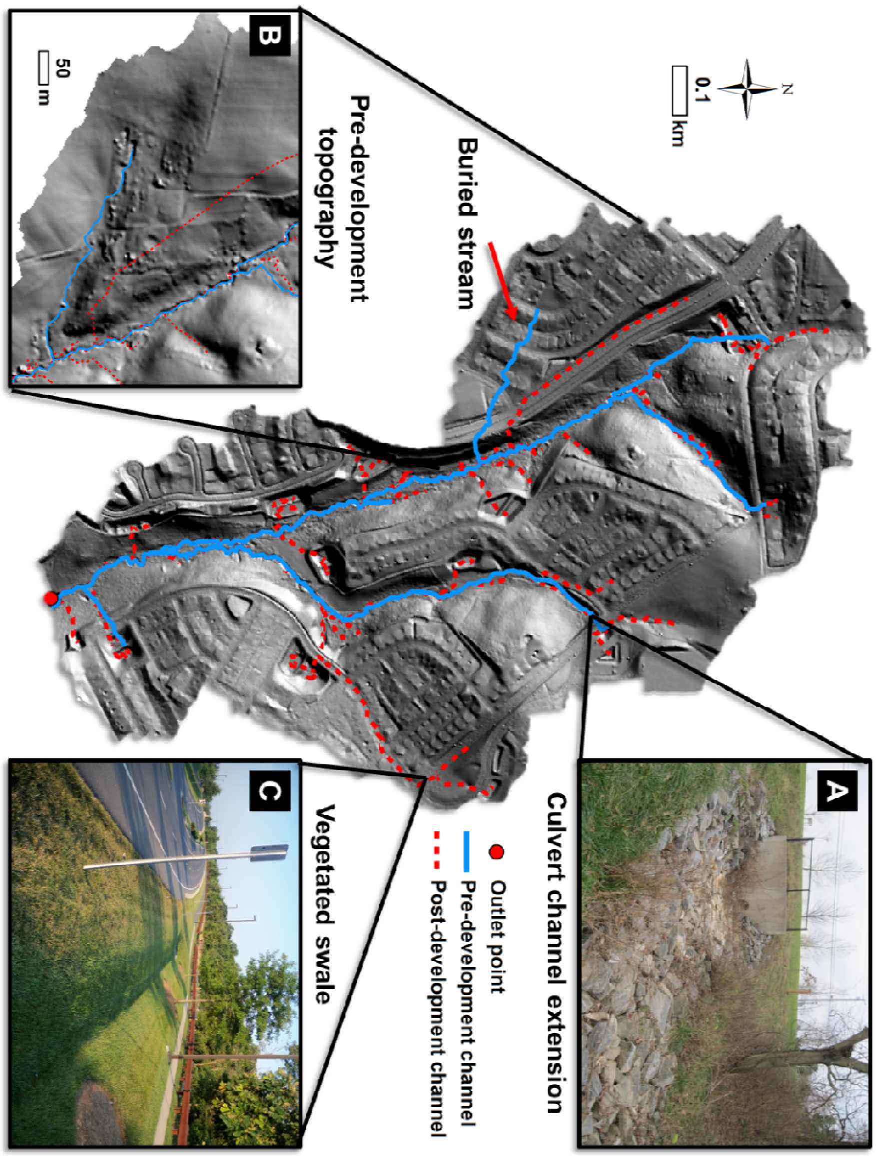
N
0.1 km
Buried stream
B
Pre-development topography
50 m
A
Culvert channel extension
Outlet point
Pre-development channel
Post-development channel
C
Vegetated swale

Tracking geomorphic signatures of watershed suburbanization with multitemporal LiDAR

Daniel K. Jones[a,b *], Matthew E. Baker[b,1], Andrew J. Miller[b,2], S. Taylor Jarnagin[c,3], Dianna M. Hogan[a,4]

[a]U.S. Geological Survey, Eastern Geographic Science Center, 12201 Sunrise Valley Drive, Reston, VA 20192, USA

[b]Department of Geography and Environmental Systems, University of Maryland, Baltimore County, Sondheim Hall, 1000 Hilltop Circle, Baltimore, MD 21250, USA

[c]U.S. Environmental Protection Agency (USEPA) Landscape Ecology Branch, Environmental Sciences Division, USEPA/ORD National Exposure Research Laboratory, Mail Drop E243-05 109 T.W. Alexander Drive, Research Triangle Park, NC 27711, USA

*Corresponding author. Present address: U.S. Geological Survey, Eastern Geographic Science Center, 12201 Sunrise Valley Drive, Reston, VA 20192, USA; Tel.: +1 (703) 648-5120; Fax: +1 (703) 648-4603; E-mail: dkjones@usgs.gov.

[1]E-mail: mbaker@umbc.edu.
[2]E-mail: miller@umbc.edu.
[3]E-mail: jarnagin.taylor@epa.gov.
[4]E-mail: dhogan@usgs.gov.

Abstract

Urban development practices redistribute surface materials through filling, grading, and terracing, causing drastic changes to the geomorphic organization of the landscape. Many studies document the hydrologic, biologic, or geomorphic consequences of urbanization using space-for-time comparisons of disparate urban and rural landscapes. However, no previous studies have documented geomorphic changes from development using multiple dates of high-resolution topographic data at the watershed scale. This study utilized a time series of five sequential Light Detection and Ranging (LiDAR) derived digital elevation models (DEMs) to track watershed geomorphic changes within two watersheds throughout development (2002-2008) and across multiple spatial scales (0.01-1 km^2). Development-induced changes were compared against an undeveloped forested watershed during the same time period. Changes in elevations, slopes, hypsometry, and surface flow pathways were tracked throughout the development process to assess watershed geomorphic alterations. Results suggest that development produced an increase in sharp topographic breaks between relatively flat surfaces and steep slopes, replacing smoothly varying hillslopes and leading to greater variation in slopes. Examinations of flowpath distributions highlight systematic modifications that favor rapid convergence in unchanneled upland areas. Evidence of channel additions in the form of engineered surface conduits is apparent in comparisons of pre- and post-development stream maps. These results suggest that topographic modification, in addition to impervious surfaces, contributes to altered hydrologic dynamics observed in urban systems. This work highlights important considerations for the use of repeat LiDAR flights in analyzing watershed change through time. Novel methods introduced here may allow improved understanding and targeted mitigation of the processes driving

geomorphic changes during development and help guide future research directions for development-based watershed studies.

Keywords: LiDAR time series; urbanization; land cover change; digital elevation models; anthropogenic geomorphology; watershed

1. Introduction

At least one-third of the Earth’s continental surface has undergone some form of anthropogenic geomorphological activity (Rózsa, 2010). Of these activities, construction and urban development stand out as ongoing and expanding causes of geomorphic change characterized by rapid, complex, and multiscalar processes. Throughout urban development, extensive landscape grading, leveling, and terracing can change the fundamental organization of topography within a watershed (Tenenbaum et al., 2006; Csima, 2010). The current ability to track, quantify, and predict development-induced geomorphic changes is hindered by insufficient data and reliance on methodologies developed for traditional geomorphic studies in natural settings (Djokic and Maidment, 1991; Haff, 2003; Gironás et al., 2010; Rózsa, 2010; Szabo, 2010). High-resolution topographic data, such as Light Detection and Ranging (LiDAR), is required to resolve surface flowpaths and visualize roads and other fine-scale features in urban landscapes (Djokic and Maidment, 1991; Tenenbaum et al., 2006; Hunter et al., 2008; Gironás et al., 2010). Sequential topographic data sets are needed to track and quantify the multiscalar (Bochis and Pitt, 2005; Tenenbaum et al., 2006; Bochis, 2007) and temporally variable (MDE, 2000; Dietz and Clausen, 2008) topographic changes throughout development. No studies have utilized a high-resolution digital elevation model (DEM) time series to track geomorphic changes throughout the development process.

The topographic footprint of development is visually striking on the ground and from the air, highlighting large-scale landscaping carried out during initial development phases (Csima, 2010). Final smoothing and regrading occurs at finer scales that are less immediately apparent in topographic data, but are nonetheless important for understanding surficial drainage and altered geomorphic characteristics (MDE, 2000; Tenenbaum et al., 2006). How best to quantify such topographic changes is unclear in terms of selecting geomorphic variables and spatial scales that most effectively capture observed changes (Haff, 2003; Rózsa, 2010). Topographic variables such as slope, curvature, and their distribution relative to watershed area play important roles in sediment transport and erosion dynamics (Moore et al., 1991; Montgomery and Foufoula-Georgiou, 1993; James et al., 2007), channel formation (Band, 1993; Montgomery and Foufoula-Georgiou, 1993), and surface water – groundwater exchanges (Beven and Kirkby, 1979; Moore et al., 1991; Tenenbaum et al., 2006). However, topographic controls on hydrologic and geomorphic processes may be altered in urban landscapes because of infrastructure (e.g., roads, pipes) (Djokic and Maidment, 1991; Tenenbaum et al., 2006; Gironás et al., 2009; Rózsa, 2010; Choi, 2012).

Five sequential LiDAR-derived DEMs spanning the development of two small, historically agricultural watersheds were obtained to track geomorphic changes throughout development. The goal of this study is to understand how and where geomorphic changes manifest within these watersheds and to understand their implications for watershed geomorphic and hydrologic processes prior to accounting for influences of stormwater infrastructure. The DEM coverage of a third, forested reference watershed was used to track temporal variation not attributable to development. This work will introduce a number of novel methods for tracking temporal geomorphic changes using sequential LiDAR DEMs and will highlight unique geomorphic signatures of the development process. Results of this study will help guide ongoing research efforts that focus on the coupled influence of topography and infrastructure on watershed function.

2. Site description

For this study, three watersheds in Montgomery County, Maryland, within the Piedmont Physiographic Province were examined. All three watersheds are within the Mt. Airy Uplands District, characterized by siltstones and quartzite with underlying crystalline bedrock consisting of a phyllite/slate unit, with average annual precipitation of 106.4 cm (Reger and Cleaves, 2008; Hogan et al., 2014). Soper Branch (forested control) drains an area of ~ 3.4 km^2 with an overall mean gradient of 13%. Land cover is predominantly classified as deciduous forest (~ 85%) and small percentages of low-density housing and agriculture (6 and 9%, respectively) (Hogan et al., 2014; Dr. J.V. Loperfido, USGS, oral communication, July 2013). Tributaries 104 and 109 (T104 and T109, urbanizing) drain areas of ~ 1.2 and 0.9 km^2 with mean gradients of 11 and 8%, respectively. Tributaries 104 and 109 are historically agricultural watersheds that underwent extensive suburban development from 2003 to the present. Tributary 104 land use shifted from 41% agriculture, 0.3% barren, 42% forest, and 17% urban in 2002 to 2% agriculture, 15% barren, 19% forest, and 64% urban in 2008. Across the same time period, T109 changed from

64% agriculture, 1% barren, 25% forest, and 10% urban to 45% agriculture, 13% barren, 25% forest, and 17% urban (Hogan et al., 2014). Both T104 and T109 were used in analyses of development-induced geomorphic changes. However, development in T109 was not complete at the time of the last LiDAR flight, so the final T109 DEM represents a different stage of development than T104.

Tributaries 104 and 109 fall within the Clarksburg Special Protection Area (CSPA, established in 1994) and are subject to development guidelines and restrictions (Maryland DEP, 2013). Broadly speaking, the Special Protection Area designation identifies areas with high quality natural resources and requires ongoing and future development projects to implement best available water quality and quantity protection measures. Water quality and quantity measures often exceed minimum local and state regulations and include extensive Best Management Practices (BMPs) implementation during (sediment and erosion controls; S&EC) and after development (stormwater management; SWM) (Hogan et al., 2014). Each watershed has extensive storm sewer (SS) infrastructure in addition to noted BMP and SWM structures. While SS infrastructure likely plays a key role in dictating watershed hydrology, the purpose of this study is to document geomorphic changes and their hydrologic implications independent of SS influence. Ongoing research will incorporate SS infrastructure to distinguish its effects from geomorphic impacts and better account for watershed hydrologic dynamics.

3. Data description and methods

Five sequential LiDAR-derived 1-m bare-earth point clouds were collected at semiannual intervals from 2002 to 2008 to track development-induced topographic changes in T104 and T109 and background topographic changes in Soper Branch. Detailed LiDAR vendor, instrumentation, and accuracy information are provided by Jarnagin (2010). Building removal and bare-earth point cloud filtering was performed by each LiDAR vendor utilizing proprietary software, summarized in Table 1. Differences in bare-earth filtering algorithms used by different vendors may have caused interpolated topography within filtered building footprints to vary between dates. Therefore, topographic patterns within building footprints may reflect filtering artifacts and should be interpreted with a degree of uncertainty.

Insert Table 1 near here.

LiDAR was collected as part of a larger monitoring effort to track watershed changes throughout development and to document development effects on local resources through time (Jarnagin, 2008). Detailed comparisons between LiDAR spot elevations and field-surveyed elevations across a range of slope, elevation, and land use classes are reported by Gardina (2008) and Jarnagin (2010). One-meter resolution DEMs were interpolated from bare-earth point clouds using the natural neighbor interpolation algorithm (Sibson, 1981). The DEMs were then coarsened to 2-m horizontal resolution to smooth and reduce noise in the interpolated topography. All subsequent spatial analyses were performed using the interpolated 2-m DEMs in ArcMap 9.3[1] (ESRI, Redlands, CA).

[1] Any use of trade, firm, or product names is for identification purposes only and does not imply endorsement by the U.S. Government.

3.1. Elevation change

Differencing sequential DEMs has been used to estimate sediment budgets, to identify nutrient and sediment sources and sinks (Thoma et al., 2005), and to track gully evolution through time (Perroy et al., 2010). Raw difference calculations, however, do not incorporate any estimate of the error inherent across different DEMs or LiDAR vendors (e.g., they imply that all observed elevation differences are real). Further, LiDAR precision has been shown to vary across land cover classes—with forest cover exhibiting the lowest precision (Gardina, 2008; Jarnagin, 2010). Therefore, comparisons of absolute elevation change estimates across differing land cover classes may be misleading.

To correct for the inherent variability in elevation estimates through time, DEM differences were expressed as standard deviations (SD) through time calculated for each pixel in each watershed as

$$SD = \sqrt{\frac{1}{N}\sum_{i=year}^{N}(x_i - \mu)^2} \tag{1}$$

where N is the number of DEM years (5), x_i is the elevation for a given pixel x in year i, and μ is the mean elevation of pixel x across the five DEM years. The distribution of elevation SDs in Soper Branch was then used to quantify background elevation variability in T104 and T109. The SD distribution in Soper Branch was filtered to exclude all known areas with recent anthropogenic activities or structures to assure the distribution of SDs were indicative of the background signal. Any remaining non-zero SD in Soper Branch was assumed to be attributable to either natural causes or uncertainty in the LiDAR data. Because of the decreased elevation precision observed within forested pixels (e.g., Gardina, 2008; Jarnagin, 2010), the use of Soper Branch to quantify background LiDAR variability was a conservative baseline for detecting change in nonforest areas. To detect elevation changes associated with the development process, resulting SD maps were classified based on the distribution of SDs in Soper Branch, with an additional class added to distinguish SD values outside of the range observed in Soper Branch. Classes represent SD values less than or equal to the mean, within three standard deviations of the mean, and SD values greater than three standard deviations from the mean. Any elevation change above the maximum SD observed in Soper Branch is assumed to be attributable to the development process.

3.2. Slope change

The distribution of local slopes from before and after development in T104 were quantified and classified to ranges relevant to landscape development decisions described by Csima (2010; Table 2). Each slope class in the pre-development landscape provides an indication of the relative development costs and earth-moving practices used across the watershed. A representative cross section was extracted for pre- (2002) and post- (2008) development years to highlight changes in the juxtaposition of high and low sloping areas and to differentiate spatial patterns associated with modified and unmodified areas. More broadly, changes in local terrain created by reallocating and relocating slopes were mapped using areal standard deviations of slope within a 10 x 10 pixel square neighborhood of every focal pixel x_i. Comparison of maps resulting from pre- and post-development DEMs further highlighted changes in the variability of local landscapes associated with development practices.

Insert Table 2 near here.

3.3. Hypsometric curves

Hypsometric curves represent the proportion of a watershed's area (*a/A*) that is above a given elevation (*h/H*), providing a generalized approximation of hillslope shape within the watershed. Traditionally, hypsometric curves have been used in discussions of landscape evolution across broad spatial extents (e.g., Strahler, 1957). Other studies have found hypsometric curve shape indicative of dominant erosional mechanisms (Harlin, 1980; Luo, 2000), hydrologic response (Luo and Harlin, 2003), and infiltration dynamics (Vivoni et al., 2008). Hypsometric curves were generated for each DEM year based on first-order catchment and full watershed scales to compare and contrast hillslope topographic alterations at increasingly broader spatial extents. Consistent boundaries were used for each year to assure that any hypsometric variability through time was attributable to topographic changes and not to boundary shifts caused by topographic modification along drainage divides. Hypsometric curves for each year were compared to assess hillslope level changes through time. A map of net fill and excavation (DEM_{2008} – DEM_{2002}) was also developed to help interpret hypsometric trends.

3.4. Drainage network change

Topographically based drainage network delineation methods are widely used across a range of land covers and climates. The most common approaches rely on threshold relationships of derivative watershed properties (e.g., drainage area, slope – area relationship) to define upslope channel extents (e.g., O'Callaghan and Mark, 1984; Montgomery and Foufoula-Georgiou, 1993). Other techniques utilize local topography to extract convergent drainage features and stream heads directly (e.g., plan/profile curvature) but have seen much less use because of higher topographic data resolution required for feature detection (Tribe, 1992; Band, 1993; Tarboton and Ames, 2001; Lindsay, 2006). A number of threshold-type approaches have been shown to provide reasonable approximations of field-surveyed channel networks (extent and complexity) (Heine et al., 2004; James et al., 2007; James and Hunt, 2010). However, threshold-based methods are insufficient for determining the location and occurrence of artificial urban conduits (e.g., swales, gutters) whose location is based on design specifications, not physical processes (Gironás et al., 2010; Jankowfsky et al., 2012).

Topographic openness (a measure of tangential curvature; see Yokoyama et al., 2002) was employed to identify surface networks in the pre-development terrain of T104 and then applied to the post-development terrain to compare surface network changes. Topographic openness is an angular relation of horizontal distance to vertical relief, calculated from above (positive/zenith) and below (negative/nadir) a topographic surface (DEM). For an angle < 90°, openness is equivalent to the internal angle of an inverted cone, its apex at the focal DEM pixel, constrained by neighboring elevations within a specified radial distance. Topographic openness is more robust in identifying surface convexities and concavities than commonly used profile and plan curvature (Yokoyama et al., 2002) and has been successfully applied to LiDAR to identify convergent topography (Molloy and Stepinski, 2007; Sofia et al., 2011). Topographic openness was calculated using an Arc Macro Language (AML) script (written by M.E. Baker, UMBC, personal communication, 2005) that reproduces the methods detailed in Yokoyama et al. (2002). The AML extracts DEM values for all relevant cells in a neighborhood set for each focal pixel x_i (defined by stepwise increments of one pixel width in each of eight azimuth directions until a specified search radius is reached; here we used 100 m) in a landscape. For each increment, the horizontal distance from and elevation above the focal pixel is calculated, and an arctan function converts opposite:adjacent ratios to angular degrees. The AML tracks a running maximum and minimum angle across each radial increment and all smaller increments for all eight directions, converts the resulting maxima and minima to zenith and nadir angles, and computes the mean of each across all eight directions. Thus the final openness values represent the averaged openness measure for all eight azimuths across the specified search radius.

Difference DEMs and orthoimagery were used to identify detention basins and other potential barriers to surface flow. Pre- and post-development DEMs were filled to overcome internal drainages (i.e., ’pits‘) and then subtracted from unfilled DEMs to assess filling extents. Paths were carved from detention basin low points to the next downslope pixel of equal or lesser elevation outside of the filled zone. Where possible, carved pathways followed detention basin outlets identified from areal and ground surveys. No attempt was made to account for flowpaths within internal drainage basins or subsurface drainage infrastructure. Straight-line pathways were enforced for all unknown detention basin outlets. Flow directions were calculated for each year from the pit-resolved DEMs by enforcing drainage from each DEM pixel to the adjacent or diagonal pixel with the greatest drop in relief (see O'Callaghan and Mark, 1984). Resulting flow direction surfaces were used to generate drainage networks and other derivative surfaces.

To create a stream map, orthoimagery and hillshaded DEMs were overlain with openness grids to determine the critical openness for identifying surface depressions in the pre-development T104 DEM. A negative openness (nadir) angle of 91.5° was determined to sufficiently capture all visible surface depressions. All pixels at or above 91.5° were identified, and then connected using a D8-based accumulation operation to enforce downslope continuity from each depression (Tarboton and Baker, 2008). The pre-development stream map (as defined by downslope accumulation of depression pixels) was then tested for agreement with the constant drop law, which states that the mean elevation drop across channels within a given Strahler order should not be significantly different from the mean drop in the next higher order (Tarboton et al., 1991). Incremental accumulation thresholds of depression pixels were used to prune the pre-development stream map until it satisfied the constant drop law. The pre-development accumulation threshold was then applied to the post-development depression accumulation map to define the post-development stream map. Pre- and post-development stream maps were overlain and compared to assess network changes. Field visits were also conducted to classify channels as either natural (defined banks, sorted bedload, evidence of ongoing or recent flow) or artificial (e.g., swales, outflow pipes, rip rap).

4. Results

Hillshades of each DEM year highlight the spatial pattern of surface modifications incrementally throughout development (Fig. 1). Initial large-scale resurfacing throughout the watershed is clear in 2004 and 2006 hillshades, with urban or suburban infrastructure distinguishable in the terrain. Fine-scale grading and smoothing that is much less visually apparent in the LiDAR characterize late-stage development in 2006 and 2008. Valley burial is evident in the western portion of the watershed (see red arrow in Fig. 1), replaced by a smooth upland housing cluster and roadway. Mainstem valley form remained relatively constant throughout the time series, with little to no visual evidence of lateral channel movement.

Insert Figure 1 near here.

4.1. Elevation standard deviations

Pixelate elevation standard deviations (SD) calculated across the five DEM years were approximately normally distributed in Soper Branch with a mean of 0.063 m and a standard deviation of 0.034 m, ranging from 0.002 to 0.870 m. Areas with temporal SDs greater than or equal to three standard deviations of the watershed mean (≥ 0.163 m) were focused within riparian zones at or near stream banks and near the basin outlet within a relatively flat and wide floodplain area (Fig. 2). Jarnagin (2010) reported similar LiDAR errors within densely vegetated riparian zones in comparisons between ground-truth and LiDAR spot elevations (absolute mean difference of 0.216 m with a standard deviation of 0.723 m and a maximum difference of 1.180 m). Moderately high SDs (0.063-0.163 m) are also apparent on northeast- (NE) facing hillslopes. The temporal variation observed on NE-facing slopes was greater than systematic errors reported for ground survey and LiDAR-derived elevations, which exhibited a mean absolute difference of ~ 0.05 m (Gardina, 2008).

Elevation changes in T104 and T109 classified to the distribution of temporal SDs in Soper Branch highlight large areas exhibiting substantial elevation changes greater than the variability observed in forested controls. White areas in T104 and T109 signify temporal elevation SD values that are above the maximum observed in Soper Branch (> 0.870 m), encompassing ~ 24.4% and 9.9% of total watershed area, respectively. Distinct patches of high elevation variability are primarily located in development parcels evident in the post-development hillshades (2008 panel in Fig. 1). High temporal variability (0.163-0.870 m) is also apparent along the mainstem channel of T104 but is less evident in T109. Relatively low temporal SD values in the southern undeveloped portion of T109 and within riparian zones in T104 reflect magnitudes of temporal variability similar to those observed in Soper Branch. Such heterogeneous distribution of elevation change is consistent with the observation that earth-moving practices were not spatially uniform across developing parcels.

Insert Figure 2 here.

4.2. Slopes

The footprint of development is clearly distinguishable from unmodified hillslopes in a visual comparison of pre- and post-development slope maps (Fig. 3). Development created abrupt slope changes in the landscape, replacing relatively smooth topographic profiles (i.e., gray boxes in inset). Moderate to high slope classes (> 12%) were present along roads, housing parcels, and stormwater management features, despite the use of bare-earth LiDAR with buildings removed by filtering. Valley infill is apparent in the slope transect between points *a* and *b* at ~ 180 m with no evidence of the original valley structure in the post-development topography. High-frequency variation between low slope and high slope features is evident in the slope transect between 420 and 580 m across a developed subdivision.

Insert Figure 3 here.

Areal slope standard deviations calculated using a 10 x 10 pixel moving window show a marked increase in the spatial variability of local slope values in post-development topography (Fig. 4). The overall distribution of variation in local slopes exhibited a positive shift from the pre- (mean areal slope standard deviation of 2.35 ± 2.26%) to post-development terrain (mean areal slope standard deviation of 4.69 ± 3.54%). Highly variable slope zones in 2002 were limited to riparian corridors and preexisting development plots in the northern section of T104. By contrast, post-development slopes exhibit greater local variation (i.e., steeper and flatter terrain in close proximity) associated with the grading of subdivisions and road embankments.

Insert Figure 4 here.

4.3. Hypsometry

Despite substantial topographic changes across the watershed visible in hillshades and slope maps representing different stages of development, hypsometric changes towing to development only manifest when observed across small extents with relatively uniform, high magnitude surface changes (Fig. 5). Distinctly terraced hypsometric curves appear in the end-development phase topography, mirroring abrupt slope changes along roadways and surrounding housing parcels (see insets A and C in Fig. 5). Valley infill in subwatershed A (see red arrow in Fig. 1) created a sharp elevation gradient to the remaining riparian lowlands, reflected in the 2007 and 2008 hypsometric curves. Terracing and leveling of upslope transportation corridors also contribute to the terraced hypsometric form. Hypsometric trends of the larger subwatershed B and at the full watershed scale (D) did not exhibit detectable temporal changes.

Insert Figure 5 here.

4.4. Drainage network changes

Substantial redistribution of overland flowpaths is evident in comparisons of pre- and post-development flow direction grids (Fig. 6). As with slope comparisons, the most drastic changes in flow directions are focused along roadways and within housing parcels. Small patches of uniform flow directions mirroring housing and road footprints have replaced large, contiguous patches of homogenous flow directions (i.e., parallel flow lines) on upland hillslopes. Fine-scale variation in flow directions within relatively minor elevation change zones (see elevation change inset in Fig. 6) are coupled with more dramatic modifications within drainage features and near infrastructure. As a result of these alterations to the flow field, flow accumulation distributions exhibited a negative shift, with accumulation quartiles decreasing from 4, 11, and 29 pixels in 2002 to 1, 4, and 12 pixels in 2008. Distributional shifts reflect drainage dissection and the fragmented flow field apparent in Fig. 6 with small, locally convergent pathways replacing large, contiguous, parallel flowpaths.

Insert figure 6 here.

A depression pixel (openness ≥ 91.5º) accumulation threshold of three pixels was found to satisfy the constant drop criterion in the pre-development terrain of T104. The three-pixel threshold was then applied to the post-development terrain to evaluate surface network changes. Comparisons of pre- and post-development drainage network structure in T104 indicate a net gain in stream length of 4.25 km (~ 52% increase) throughout the watershed (Fig. 7). Additions were common along transportation infrastructure as swales or gutters typical in this watershed. Upslope extensions of existing channels also occurred extending beyond preexisting piped infrastructure at the apparent head of pre-development drainage lines (Fig. 7A). Valley infill (see Fig. 6A) caused the loss of a tributary but was replaced by an artificial conduit that paralleled a nearby road (Fig. 7B). Similar conduits are apparent on the eastern side of the watershed as well (Fig. 7C). No substantial changes were apparent in the mainstem channel as suggested by the near 1:1 overlap in pre- and post-development networks.

Insert Figure 7 here.

5. Discussion

The growing footprint of development in T104 is clearly visible in the DEM hillshade time series, with distinct early- and late-stage development phases operating at unique spatial scales (Fig. 1). Large-scale cutting and filling to support major infrastructure characterizes early development, evident in the 2004 and 2006 hillshades. In contrast, fine-scale leveling and grading of housing parcels characterize late-stage development (MDE, 2000). Fine-scale earth-moving practices are less immediately apparent in hillshades but are detectable in derivative data sets, as this study has shown. Results show that geomorphic changes associated with urban development are significant and nonuniform and could have implications for management and conservation efforts.

Initial analysis of background elevation changes in Soper Branch revealed nonzero standard deviations focused on northeast- (NE) facing hillslopes and within riparian and floodplain areas (Fig. 2). Increased variation on NE hillslopes may reflect flight paths taken during LiDAR collection or possible aspect differences in vegetation and soils. Slightly lower systematic errors reported in Gardina (2008) were attributed in part to methods used to derive bare-earth point clouds and, in part, to LiDAR system error. The NE artifact likely is a combination of vegetation and LiDAR system errors. Riparian and floodplain variability in Soper Branch can be attributed to LiDAR errors reported by Jarnagin (2010). In comparisons between LiDAR elevations and field-surveyed spot elevations, Jarnagin observed greater LiDAR error in densely vegetated riparian zones and on steep slopes common around incised channels. Distinguishing temporal variability attributable to artifacts in the LiDAR time series was necessary before reaching any quantitative conclusions about topographic changes resulting from development.

Elevation standard deviations classified to distinguish background and development-induced changes clearly show that earth moving in T104 and T109 was nonetheless substantially greater than background geomorphic changes observed in Soper Branch. Magnitudes similar to temporal standard deviations found in Soper Branch were observed in T104 across preexisting housing parcels and riparian zones left untouched to comply with riparian protection policies. Somewhat higher variability observed along the mainstem channel in T104 may indicate subtle channel shifts and bank erosion throughout the time period despite attempts to insulate the channel from the hydrologic and geomorphic effects of development. Also, some of the observed elevation changes may possibly reflect artifacts produced by removing buildings from the raw LiDAR point clouds. Because of the proprietary nature of the LiDAR processing, evaluating the bare-earth detection algorithms used by the data providers was not possible for this study.

Surface changes throughout development in T104 and T109 altered slopes to support infrastructure, enforce drainage, and promote infiltration. Comparison of pre- and post-development slope maps in T104 shows a marked increase in high slope classes with development as well as reallocation across space (Fig. 3). High slope classes focused along transportation corridors and surrounding detention basins are likely to promote surface drainage. Slopes leading toward streams in the pre-development map appear to steepen with development as well, likely reflecting upland filling and terracing. Stream burial is a frequently cited phenomenon in urban watersheds (Leopold et al., 2005; Elmore and Kaushal, 2008; Roy et al., 2009; Doyle and Bernhardt, 2011) and is apparent on the western side of T104 (~ 180 m in transect inset of Fig. 3). However, without infrastructure design documents it is difficult to determine whether the stream is piped under its original flowpath or if it has been redirected to flow alongside the nearby road running north to south.

Regular shifts between high and low slopes within subdivisions likely reflect housing parcels (low slopes) separated by graded lawns and swales (higher slopes) to promote drainage (Fig. 4). Low slopes within building footprints reflect the building removal algorithm applied to LiDAR point clouds to extract bare-earth points used in this study to create DEMs. The spatial distribution of high and low slopes in part controls the spatial distribution of runoff generation and infiltration zones (Beven and Kirkby, 1979; Tenenbaum et al., 2006). Shifts in the spatial pattern and magnitude of slopes may contribute to altered watershed processes including runoff generation, nutrient and sediment transport, and surface water – groundwater exchanges.

Hypsometric trends within small subwatersheds of T104 appear to mirror aforementioned steepening of valley walls with development (Fig. 5). Upland filling and grading further exacerbates the disparity in elevations between the now-developed uplands and the riparian lowlands. Redistribution of flowpaths at and around valley infills likely altered surface and subsurface water exchanges, thus changing the functional connectivity of upland and lowland areas. Dynamics are further complicated by stormwater management infrastructure, such as detention ponds and infiltration trenches, typically located between upland (development plots) and lowland (riparian zone) areas to capture and treat overland runoff before it enters local streams (Montgomery County Planning Department, 1994). Thus, riparian areas may no longer be functionally connected to upland areas during rain events unless stormwater management outfalls are triggered. Further research is required to investigate the nature of the altered surface

– groundwater connections. Lack of temporal trends in the larger subwatershed topography or throughout the entire watershed result from spatial averaging and may indicate a detection limit for tracking parcel or block-level topographic change with hypsometry.

Development caused a substantial reconfiguration of overland flowpaths from large contiguous areas of uniform directions to small, spatially fragmented patches (Fig. 6). The nonrandom distribution of smaller patches mirrors housing footprints, transportation corridors, and stormwater management infrastructure and reflects landscape-engineering practices that promote efficient collection and drainage of overland runoff (Fig. 7). Adjacent pixels with uniform directions indicate parallel flowpaths, which will not converge until a pixel with a differing direction is encountered downslope (O'Callaghan and Mark, 1984). By introducing heterogeneity into the flow direction surface, development has created both more dissected subbasins and increased opportunities for small flowpaths to converge. Increased convergence in upland areas causes overland flow to reach moderately low accumulations more often and very high accumulations more rarely than in the pre-development terrain. Decreased median and first-quartile values between 2002 and 2008 reflect the dominance of low accumulation pathways with development. Such alterations are likely the cumulative result of many site-specific efforts to increase local water conveyance, but their cumulative effect should also have implications for patterns of soil moisture, variable source area, erosion, infiltration, and recharge (Beven and Kirkby, 1979; Moore et al., 1991; Tenenbaum et al., 2006). To our knowledge, a geomorphic driver of increased upland convergence in developed terrain has yet to be described in the literature. Typically, pipes and impervious surfaces are thought to be the causal agents of altered runoff, nutrient, and sediment dynamics in urban watersheds (e.g., Paul and Meyer, 2001; Dietz and Clausen, 2008; Roy et al., 2008). However, our results indicate that the geomorphic modifications that occur with development are substantial and could also contribute to altered watershed functions.

Comparisons of pre- and post-development drainage networks reveal channel additions through engineered surface conduits (e.g., swales, culverts) and losses caused by valley infill or subsurface routing (Fig. 7). Despite noted variability in elevations along stream banks, only minor shifts were apparent in the mainstem of T104. Results of this study also raise questions about what constitutes a channel in an urban landscape. Traditional channel definitions, characterized by defined banks and sorted bedloads (Montgomery and Dietrich, 1989; Heine et al., 2004) exclude engineered surface conduits that become active during precipitation events (Doyle and Bernhardt, 2011). Excluding these artificial conduits and subsurface stormwater pipes may underrepresent the surficial connectivity of urban watersheds. Without infrastructure design documents, the true drainage connectivity of the watershed is unclear. Ongoing work will explore methods for incorporating subsurface drainage features into T104 network representations (e.g., Gironás et al., 2009; Choi, 2012; Jankowfsky et al., 2012) and determine how best to incorporate BMP infrastructure into predicted network representations. Nevertheless, this study indicates an overall increase in surface connectivity with development independent of changes in impervious surface cover or subsurface stormwater infrastructure. Increased connectivity would result in faster and larger storm peaks if left unchecked by stormwater management infrastructure. Therefore, considering geomorphic changes in addition to impervious surface cover impacts is important for remediation efforts in urban areas.

6. Conclusions

This study has shown the utility of sequential LiDAR-derived DEMs for tracking and quantifying the geomorphic changes associated with development. Using a forested watershed as a reference, background topographic variability was quantified and differentiated from development-induced topographic change. Utilizing first- and second-order topographic derivatives, this study demonstrated that development generates increasingly disjointed hillslopes characterized by abrupt slope changes separating flat upland areas. Temporal variation in elevations, slopes, and hypsometric curves likely contributes to altered watershed functions, but further research is required to understand their importance relative to stormwater infrastructure. Substantial modification of overland flowpaths resulted in subtle changes to delineated network structure, highlighting additions and losses to the pre-development network. This study's ability to detect natural and manmade ephemeral surface conduits provides a more complete accounting of watershed hydrologic connectivity. Better accounting of upslope ephemeral channel extensions may help in designating areas for protection in future development projects. The geomorphic signal of increased landscape convergence and drainage density indicates more rapid runoff generation and conveyance independent of impervious surface cover or storm sewers. A better understanding of how and where geomorphic changes occur throughout development may enable a better understanding of pollutant mobilization and retention processes. Ongoing work seeks to incorporate known subsurface pipe and BMP structures into surface network representations to understand watershed hydrologic response dynamics.

Results presented here raise important considerations for temporal topographic studies. Standard topographic methods developed for use in larger, mostly nonurban watersheds (e.g., DEM differencing, hypsometry) have limited applicability for tracking urbanization unless summarized across a relatively small extent. Additional research is needed to gain a better understanding and to develop novel methods for tracking and quantifying urban topographic modifications.

Acknowledgements

LiDAR funding provided in part by the U.S. Environmental Protection Agency under contract number EP-D-05-088 to Lockheed Martin. The U.S. Environmental Protection Agency through its Office of Research and Development collaborated in the research described here. This manuscript has been subjected to Agency review and approved for publication. This work would not have been possible without the Clarksburg Integrated Study Partnership, which includes the U.S. Environmental Protection Agency Landscape Ecology Branch (USEPA LEB), Montgomery County Department of Environmental Protection (DEP), the U.S. Geological Survey Eastern Geographic Science Center (USGS EGSC), the University of Maryland (UMD), and the University of Maryland, Baltimore County (UMBC). We would like to thank Adam Bentham and one anonymous referee for providing constructive feedback on our paper during the review process.

References

Band, L.E., 1993. Extraction of channel networks and topographic parameters from digital elevation data. In: Beven, K.J., Kirkby, M.J. (Eds.), Channel Network Hydrology. Wiley, New York, NY, pp. 13-42.

Beven, K.J., Kirkby, M.J., 1979. A physically based, variable contributing area model of basin hydrology. Hydrological Sciences Bulletin 24(1), 43-69.

Bochis, E.C., 2007. Magnitude of impervious surfaces in urban areas. M.S. Thesis, University of Alabama, Tuscaloosa, 165 pp.

Bochis, E.C., Pitt, R., 2005. Site development characteristics for stormwater modeling. In: 78th Annual Water Environment Federation Technical Exposition and Conference, Washington, D.C., October 29-November 2. Washington, D.C., p. 37.

Choi, Y., 2012. A new algorithm to calculate weighted flow-accumulation from a DEM by considering surface and underground stormwater infrastructure. Environmental Modelling & Software 30(0), 81-91.

Csima, P., 2010. Urban development and anthropogenic geomorphology. In: Szabó, J., Dávid, L., Lóczy, D. (Eds.), Anthropogenic Geomorphology: A Guide to Man-Made Landforms. Springer, New York, NY, pp. 179-187.

Dietz, M.E., Clausen, J.C., 2008. Stormwater runoff and export changes with development in a traditional and low impact subdivision. Journal of Environmental Management 8, 7.

Djokic, D., Maidment, D.R., 1991. Terrain analysis for urban stormwater modelling. Hydrological Processes 5(1), 115-124.

Doyle, M.W., Bernhardt, E.S., 2011. What is a stream? Environmental Science & Technology 45(2), 354-359.

Elmore, A.J., Kaushal, S.S., 2008. Disappearing headwaters: patterns of stream burial due to urbanization. Frontiers in Ecology and the Environment 6(6), 308-312.

Gardina, V.J., 2008. Analysis of LIDAR data for fluvial geomorphic change detection at a small Maryland stream. M.S. Thesis, Civil Engineering, University of Maryland, College Park, 156 pp.

Gironás, J., Niemann, J.D., Roesner, L.A., Rodriguez, F., Andrieu, H., 2009. A morpho-climatic instantaneous unit hydrograph model for urban catchments based on the kinematic wave approximation. Journal of Hydrology 377, 317-334.

Gironás, J., Niemann, J.D., Roesner, L.A., Rodriguez, F., Andrieu, H., 2010. Evaluation of methods for representing urban terrain in stormwater modeling. Journal of Hydrologic Engineering 15(1), 1-14.

Haff, P.K., 2003. Neogeomorphology, Prediction, and the Anthropic Landscape. American Geophysical Union, Washington, DC, ETATS-UNIS, 12 pp.

Harlin, J.M., 1980. The effect of precipitation variability on drainage basin morphometry. American Journal of Science 280(8), 812-825.

Heine, R.A., Lant, C.L., Sengupta, R.R., 2004. Development and comparison of approaches for automated mapping of stream channel networks. Annals of the Association of American Geographers 94(3), 477-490.

Hogan, D.M., Jarnagin, S.T., Loperfido, J.V., Van Ness, K., 2014. Mitigating the effects of landscape development on streams in urbanizing watersheds. Journal of the American Water Resources Association 50(1), 163-178.

Hunter, N.M., Bates, P.D., Neelz, S., Pender, G., Villanueva, I., Wright, N.G., Liang, D., Falconer, R.A., Lin, B., Waller, S., Crossley, A.J., Mason, D.C., 2008. Benchmarking 2D hydraulic models for urban flooding. Proceedings of the ICE - Water Management 161(1), 13-30.

James, L.A., Hunt, K.J., 2010. The LiDAR-side of headwater streams mapping channel networks with high-resolution topographic data. Southeastern Geographer 50(4), 523-539.

James, L.A., Watson, D.G., Hansen, W.F., 2007. Using LiDAR data to map gullies and headwater streams under forest canopy: South Carolina, USA. Catena 71, 132-144.

Jankowfsky, S., Branger, F., Braud, I., Gironás, J., Rodriguez, F., 2012. Comparison of catchment and network delineation approaches in complex suburban environments: application to the Chaudanne catchment, France. Hydrological Processes, doi: 10.1002/hyp.9506.

Jarnagin, S.T., 2008. Collaborative research: streamflow, urban riparian zones, BMPs, and impervious surfaces. U.S. Environmental Protection Agency, Washington, D.C., EPA/600/F-08/001.

Jarnagin, S.T., 2010. Using repeated LIDAR to characterize topographic changes in riparian areas and stream channel morphology in areas undergoing urban development: An accuracy assessment guide for local watershed managers. U.S. Environmental Protection Agency, Washington, D.C., EPA/600/R-10/120, p. 167.

Leopold, L.B., Huppman, R., Miller, A.J., 2005. Geomorphic effects of urbanization in forty-one years of observation. Proceedings of the American Philosophical Society 149(3), 349-371.

Lindsay, J.B., 2006. Sensitivity of channel mapping techniques to uncertainty in digital elevation data. International Journal of Geographical Information Science 20(6), 669-692.

Luo, W., 2000. Quantifying groundwater-sapping landforms with a hypsometric technique. Journal of Geophysical Research: Planets 105(E1), 1685-1694.

Luo, W., Harlin, J.M., 2003. A theoretical travel time based on watershed hypsometry. Journal of the American Water Resources Association 39(4), 785-792.

Maryland Department of the Environment (MDE), 2000. Maryland Stormwater Design Manual. Center for Watershed Protection and the Maryland Department of the Environment, Baltimore, MD.

Maryland Department of Environmental Protection (DEP), 2013. Special Protection Areas, http://www6.montgomerycountymd.gov/dectmpl.asp?url=/content/dep/water/whatarespas.asp.

Molloy, I., Stepinski, T.F., 2007. Automatic mapping of valley networks on Mars. Computers & Geosciences 33(6), 728-738.

Montgomery County Planning Department, 1994. Clarksburg Master Plan and Hyattstown Special Study Area. Montgomery County Planning Department, Silver Spring, MD.

Montgomery, D.R., Dietrich, W.E., 1989. Source areas, drainage density, and channel initiation. Water Resources Research 25(8), 1907-1918.

Montgomery, D.R., Foufoula-Georgiou, E., 1993. Channel network source representation using Digital Elevation Models. Water Resources Research 29(12), 3925-3934.

Moore, I.D., Grayson, R.B., Ladson, A.R., 1991. Digital terrain modelling: A review of hydrological, geomorphological, and biological applications. Hydrological Processes 5(1), 3-30.

O'Callaghan, J.F., Mark, D.M., 1984. The extraction of drainage networks from digital elevation data. Computer Vision, Graphics, and Image Processing 28(3), 323-344.

Paul, M.J., Meyer, J.L., 2001. Streams in the urban landscape. Annual Review of Ecology and Systematics 32(1), 333-365.

Perroy, R.L., Bookhagen, B., Asner, G.P., Chadwick, O.A., 2010. Comparison of gully erosion estimates using airborne and ground-based LiDAR on Santa Cruz Island, California. Geomorphology 118, 288-300.

Reger, J.P., Cleaves, E.T., 2008. Draft physiographic map of Maryland and explanatory text for the physiographic map of Maryland. Maryland Geological Survey Open File Report 08-03-01.

Roy, A.H., Wenger, S.J., Fletcher, T.D., Walsh, C.J., Ladson, A.R., Shuster, W.D., Thurston, H.W., Brown, R.R., 2008. Impediments and solutions to sustainable, watershed-scale urban stormwater management: lessons from Australia and the United States. Environmental Management 42, 344-359.

Roy, A.H., Dybas, A.L., Fritz, K.M., Lubbers, H.R., 2009. Urbanization affects the extent and hydrologic permanence of headwater streams in a midwestern US metropolitan area. Journal of the North American Benthological Society 28(4), 911-928.

Rózsa, P., 2010. Nature and extent of human geomorphological impact: a review. In: Szabó, J., Dávid, L., Lóczy, D. (Eds.), Anthropogenic Geomorphology: A Guide to Man-Made Landforms. Springer, New York, NY, pp. 273-290.

Sibson, R., 1981. A brief description of natural neighbour interpolation. In: Barnett, V. (Ed.), Interpreting Multivariate Data. John Wiley & Sons, New York, NY, pp. 21-36.

Sofia, G., Tarolli, P., Cazorzi, F., Dalla Fontana, G., 2011. An objective approach for feature extraction: distribution analysis and statistical descriptors for scale choice and channel network identification. Hydrology and Earth System Sciences 15(5), 1387-1402.

Strahler, A.N., 1957. Quantitative analysis of watershed geomorphology. Transactions of the American Geophysical Union 38, 913-920.

Szabo, J., 2010. Anthropogenic geomorphology: Subject and system. In: Szabó, J., Dávid, L., Lóczy, D. (Eds.), Anthropogenic Geomorphology: A Guide to Man-Made Landforms. Springer, New York, NY, pp. 3-10.

Tarboton, D.G., Ames, D.P., 2001. Advances in the Mapping of Flow Networks from Digital Elevation Data, the World Water and Environmental Resources Congress. ASCE, Orlando, Florida, May 20-24, pp. 166-175.

Tarboton, D.G., Baker, M.E., 2008. Towards an algebra for terrain-based flow analysis. In: Mount, N., Harvey, G., Aplin, P., Priestnall, G. (Eds.), Representing, Modeling and Visualizing the Natural Environment: Innovations in GIS 13. CRC Press, New York, NY, pp. 167-194.

Tarboton, D.G., Bras, R.L., Rodriguez-Iturbe, I., 1991. On the extraction of channel networks from digital elevation data. Hydrological Processes 5(1), 81-100.

Tenenbaum, D.E., Band, L.E., Kenworthy, S.T., Tague, C.L., 2006. Analysis of soil moisture patterns in forested and suburban catchments in Baltimore, Maryland, using high-resolution photogrammetric and LIDAR digital elevation datasets. Hydrological Processes 20, 219-240.

Thoma, D.P., Gupta, S.C., Bauer, M.E., Kirchoff, C.E., 2005. Airborne laser scanning for riverbank erosion assessment. Remote Sensing of Environment 95(4), 493-501.

Tribe, A., 1992. Automated recognition of valley lines and drainage networks from grid digital elevation models: a review and a new method. Journal of Hydrology 139, 263-293.

Vivoni, E.R., Di Benedetto, F., Grimaldi, S., Eltahir, E.A.B., 2008. Hypsometric control on surface and subsurface runoff. Water Resources Research 44(12), W12502.

Yokoyama, R., Shirasawa, M., Pike, R.J., 2002. Visualizing topography by openness: A new application of image processing to digital elevation models. Photogrammetric Engineering & Remote Sensing 68(3), 257-265.

List of Figures

Fig. 1. Sequential light detection and ranging (LiDAR) derived digital elevation models (DEMs) spanning the development process in T104 show the topographic footprint of development increasing through time. Boxes highlight topographic differences between early- and late-stage development practices. The red arrow denotes a valley that was buried during development.

Fig. 2. Elevation change through time quantified as temporal standard deviations (SD) calculated for each DEM pixel. Map values are classified to the distribution of elevation variation observed in Soper Branch (forested control). Black and dark gray areas represent values below and within three standard deviations of the areal mean in Soper Branch, respectively. Light gray areas represent temporal variation in elevation greater than three standard deviations above the areal mean in Soper Branch; whereas white areas are greater than the maximum, and both indicate areas of substantial development.

Fig. 3. Comparisons of pre- (2002) and post- (2008) development slope distributions in T104 classified to ranges relevant to development practices (see Table 2 after Csima, 2010). Inset

shows a cross-sectional profile of slope along the dashed red line between points *a* and *c*. Substantial differences in the variability of local slopes are evident in the profile between developed (shaded zone) and undeveloped (unshaded) parcels. High slopes ring roads, swales, and detention features and manifest as high magnitude variation across the lateral transect.

Fig. 4. Areal slope standard deviations calculated using a 10x10 pixel moving window for pre- and post-development T104 slope maps. As in pixelate slope maps, highly variable slope zones are concentrated along road corridors and around detention ponds. Nevertheless, a substantial increase in the local variability of slope is apparent in 2008, with high standard deviation values widely distributed across the watershed.

Fig. 5. Hypsometric variability through time exhibits distinctly different patterns across first-order subwatersheds in T104 (A, B, and C). Hypsometry of relatively small subwatersheds that underwent substantial resurfacing (A ~ 0.09 km^2 and C ~ 0.03 km^2) shifted from smooth (black curves) to terraced curve forms (gray curves) reflecting grading of developed parcels. However, extensive resurfacing was not apparent in hypsometric trends of larger subwatersheds (B ~ 0.43 km^2) or at the full watershed scale (D ~ 1.18 km^2).

Fig. 6. Extensive topographic modification (e.g., C) associated with grading throughout development (2002-2008) causes substantial variation in overland flowpath directions and elevation change (D) in T104. Comparisons between pre- and post-development years show that fine-scale flow direction changes at the hillslope scale are coupled with the designed orientation and gradients of road networks (A and B, with each color representing a unique direction of

overland flow). Large patches of a single color indicate parallel flow lines down a hillslope, whereas fragmentation of the 2002 map in 2008 necessarily indicates redirection and convergence of previously unconnected contributing areas.

Fig. 7. Comparison of pre- (blue lines) and post- (red dashed lines) development channel network delineations suggest increased network density with development in T104. Added channels include upslope extensions beyond existing culverts (A) and vegetated swales parallel to roadways (C). Comparisons to pre-development topography show a minor tributary that has been buried during development (B).

Table 1
Building removal and bare-earth point cloud processing information for each LiDAR year provided by S.T. Jarnagin (personal communication, 2013).[a]

LiDAR year	Instrument	Vendor	Building removal software	Bare-earth filtering
2002	Optech ALTM-2025	Airborne 1	Optech's REALM 2.27	Terrascan (running on Microstation)
2004	Optech ALTM-2033	Laser Mapping Specialists Inc.	Applanix POSPROC & Optech's REALM (versions not specified)	Spectra's Terramodel
2006	Optech ALTM-3100	Canaan Valley Institute	Optech's REALM (version not specified)	Microstation 8 with Terrascan
2007	Optech ALTM-3100	Canaan Valley Institute	Optech's REALM (version not specified)	Microstation 8 with Terrascan
2008	Leica ALS-50	Sanborn	Applanix POSPROC 4.3	Leica ALS post-processing and Terrasolid Terrascan

[a]Any use of trade, firm, or product names is for identification purposes only and does not imply endorsement by the U.S. Government.

Table 2
Slope classes and associated economic costs and considerations for urban development (adapted from Csima, 2010)

Angle of slope	Development potential and the required landscaping
Up to 5%	Easy and economic development potential. In general, terracing not necessary; landscaping exclusively restricts to drainage. Relief does not pose a limit either to buildup density or building size.
5-12%	Increased development costs. Landscaping is inevitable; development is only possible with terracing and slope leveling. Somewhat limited development.
12-25%	Development potential at significant cost and labor expenditure, only with terraces and supporting walls provided. Major topographic transformation; relief fundamentally controls the type of development to be applied.
25-35%	Limited potential for urban development. Low building density with small-sized buildings.
Above 35%	Unsuitable for urban development.

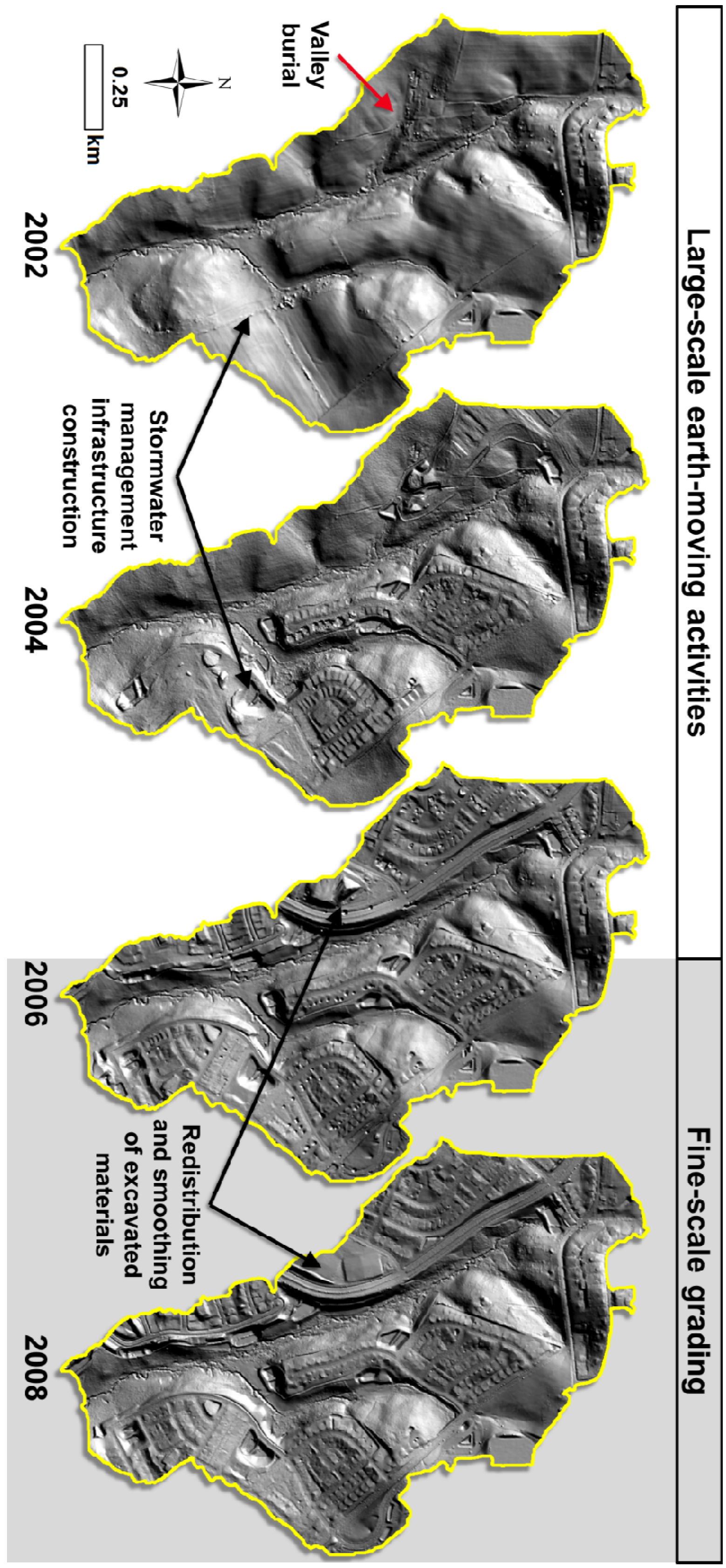

Large-scale earth-moving activities
Fine-scale grading
Valley burial
N
0.25 km
2002
Stormwater management infrastructure construction
2004
2006
Redistribution and smoothing of excavated materials
2008

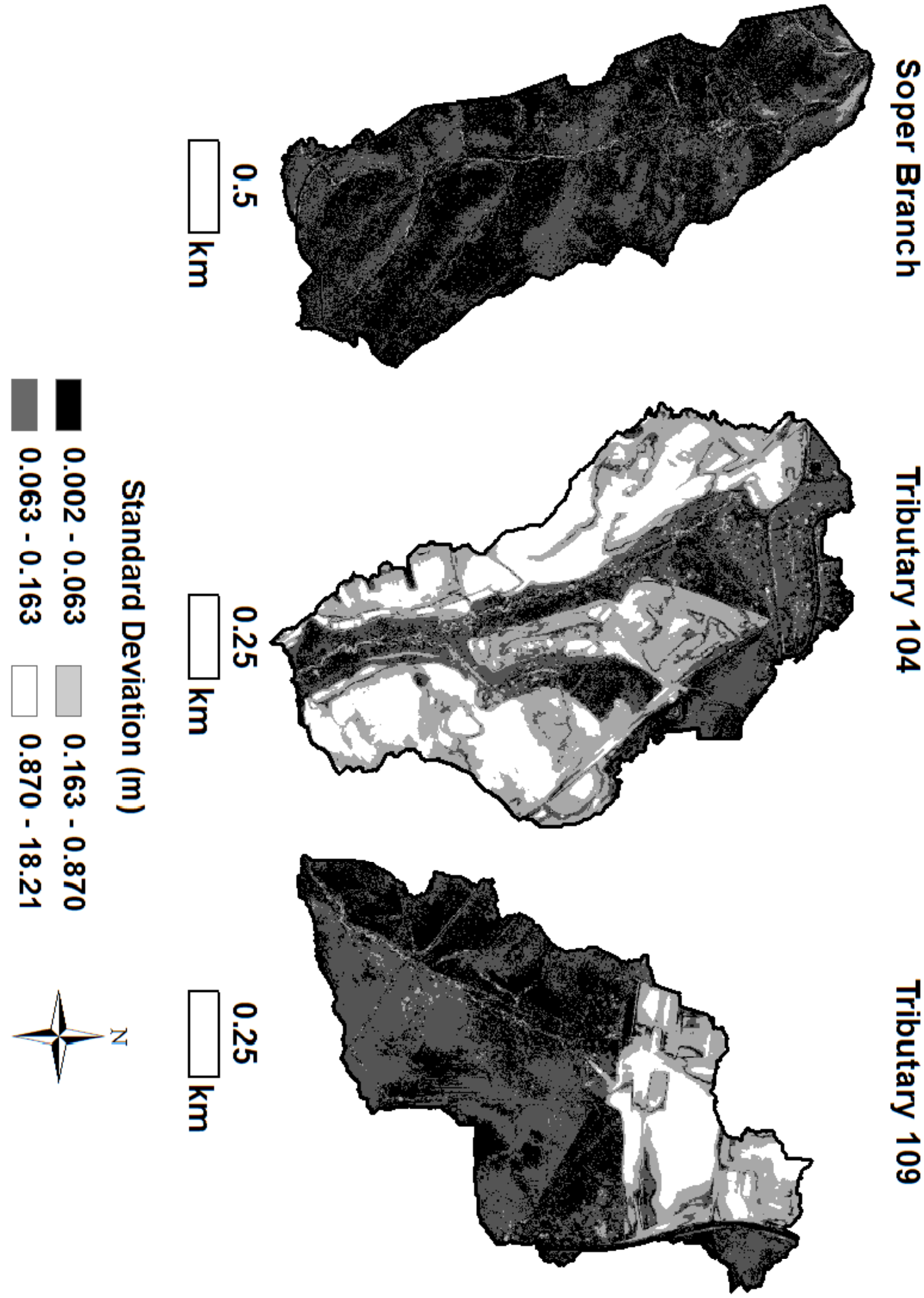
Soper Branch
Tributary 104
Tributary 109
0.5
km
0.25
km
0.25
km
Standard Deviation (m)
0.002 - 0.063
0.063 - 0.163
0.163 - 0.870
0.870 - 18.21
N

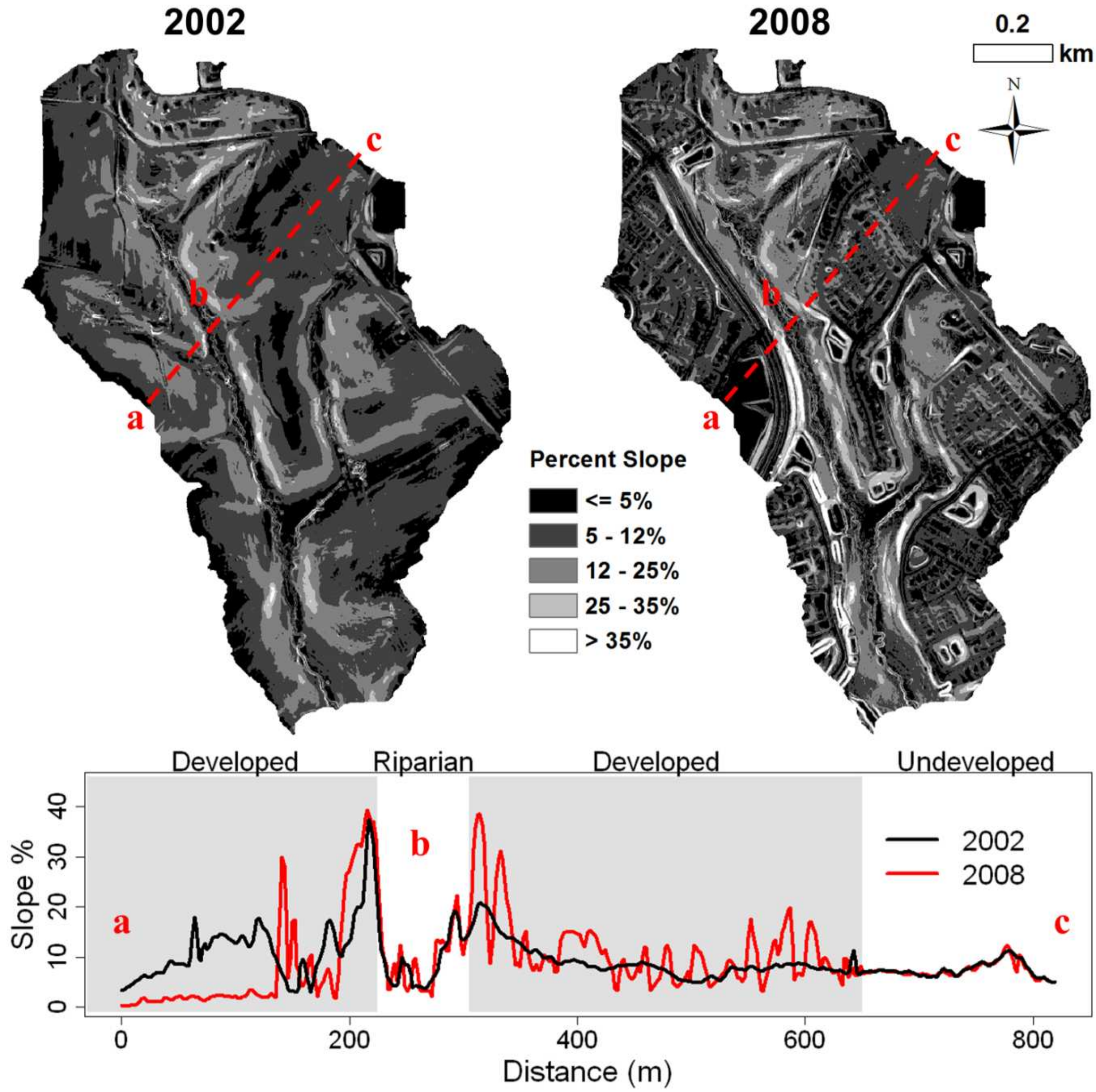
2002
2008
0.2
km
N
a
b
c
Percent Slope
<= 5%
5 - 12%
12 - 25%
25 - 35%
> 35%
Developed
Riparian
Developed
Undeveloped
Slope %
Distance (m)
0
10
20
30
40
200
400
600
800
2002
2008

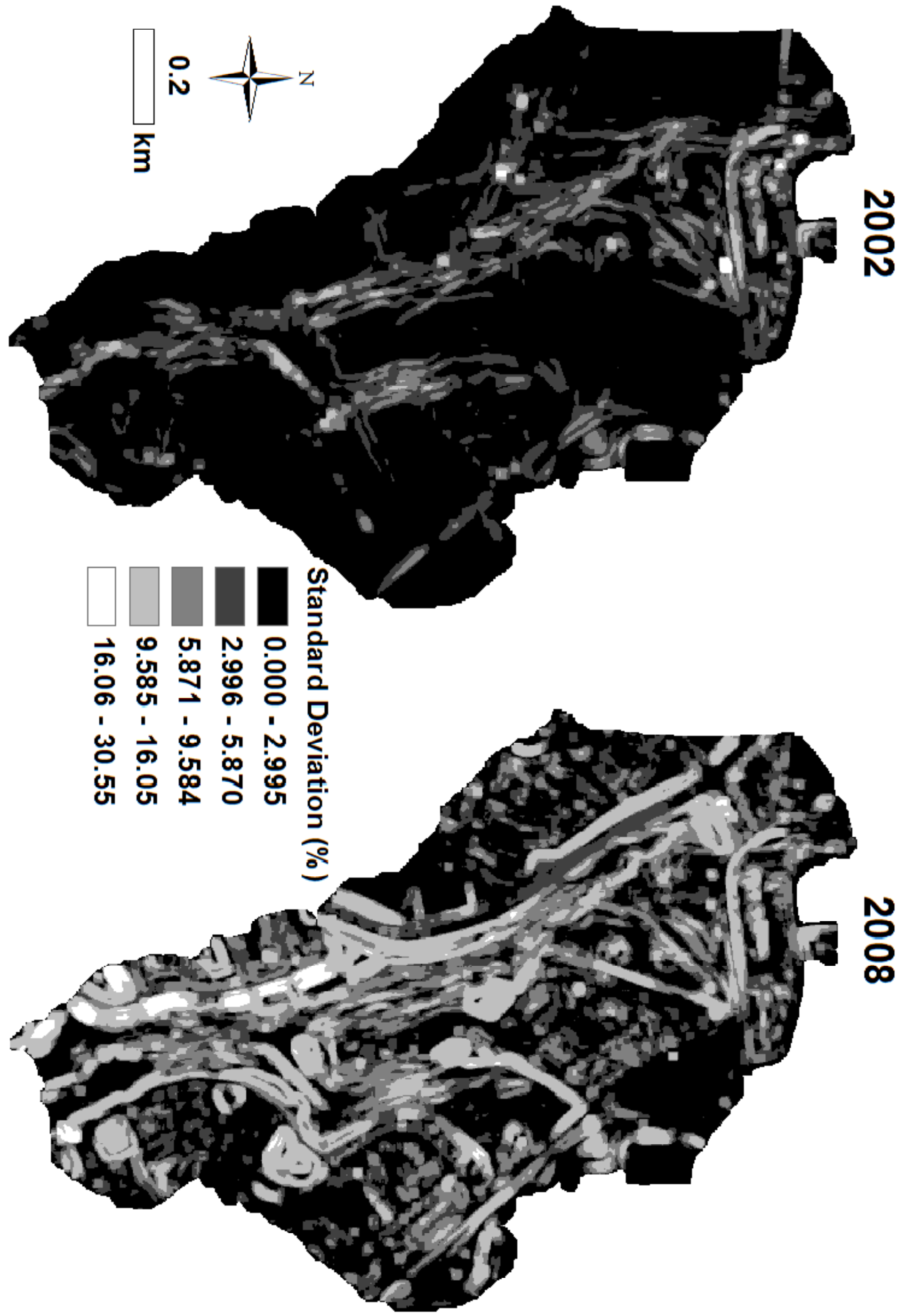
2002
2008
N
0.2
km
Standard Deviation (%)
0.000 - 2.995
2.996 - 5.870
5.871 - 9.584
9.585 - 16.05
16.06 - 30.55

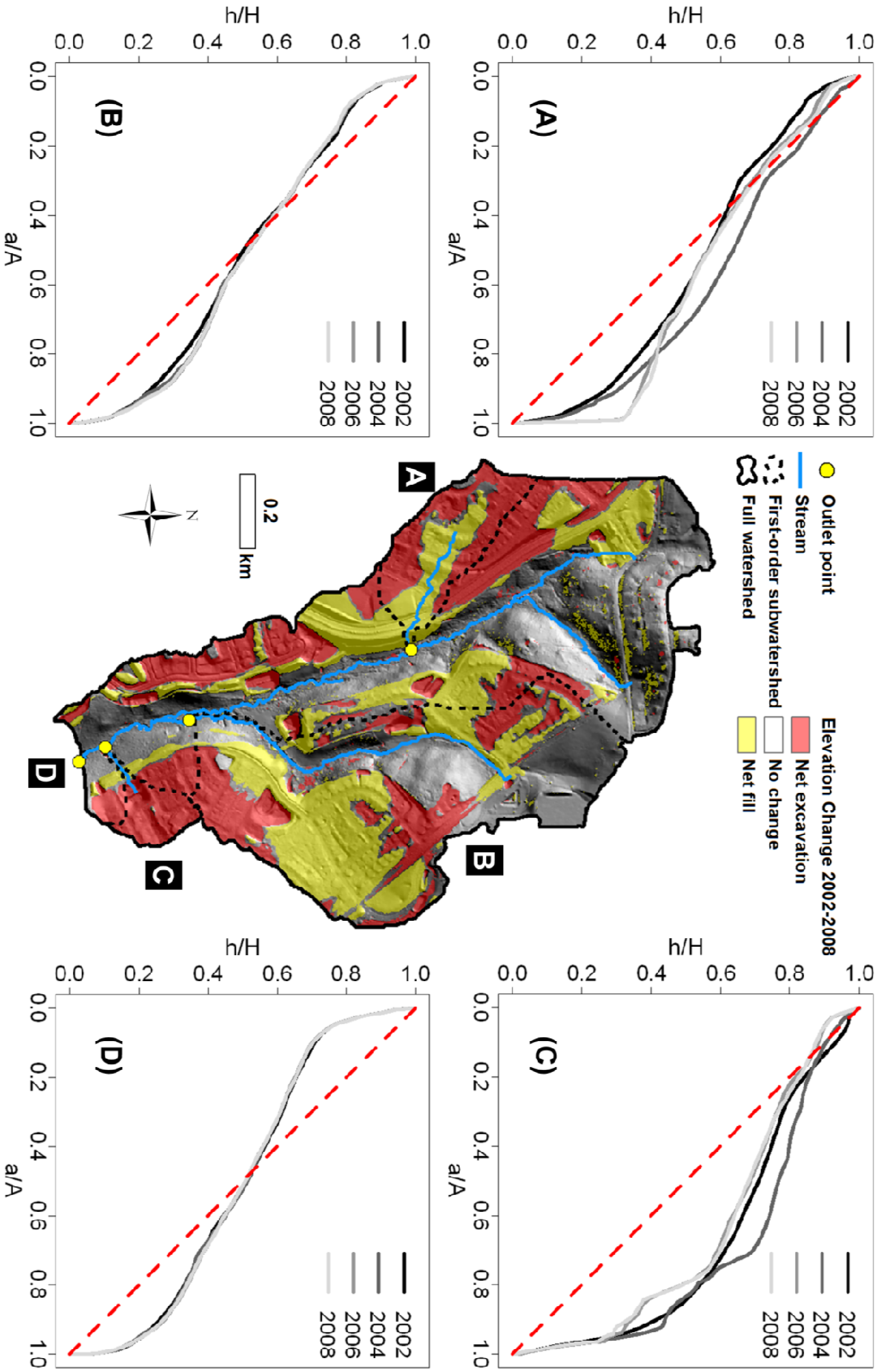
(A)
(B)
(C)
(D)
h/H
a/A
0.0
0.2
0.4
0.6
0.8
1.0
2002
2004
2006
2008
Outlet point
Stream
First-order subwatershed
Full watershed
Elevation Change 2002-2008
Net excavation
No change
Net fill
0.2
km
N
A
B
C
D

767

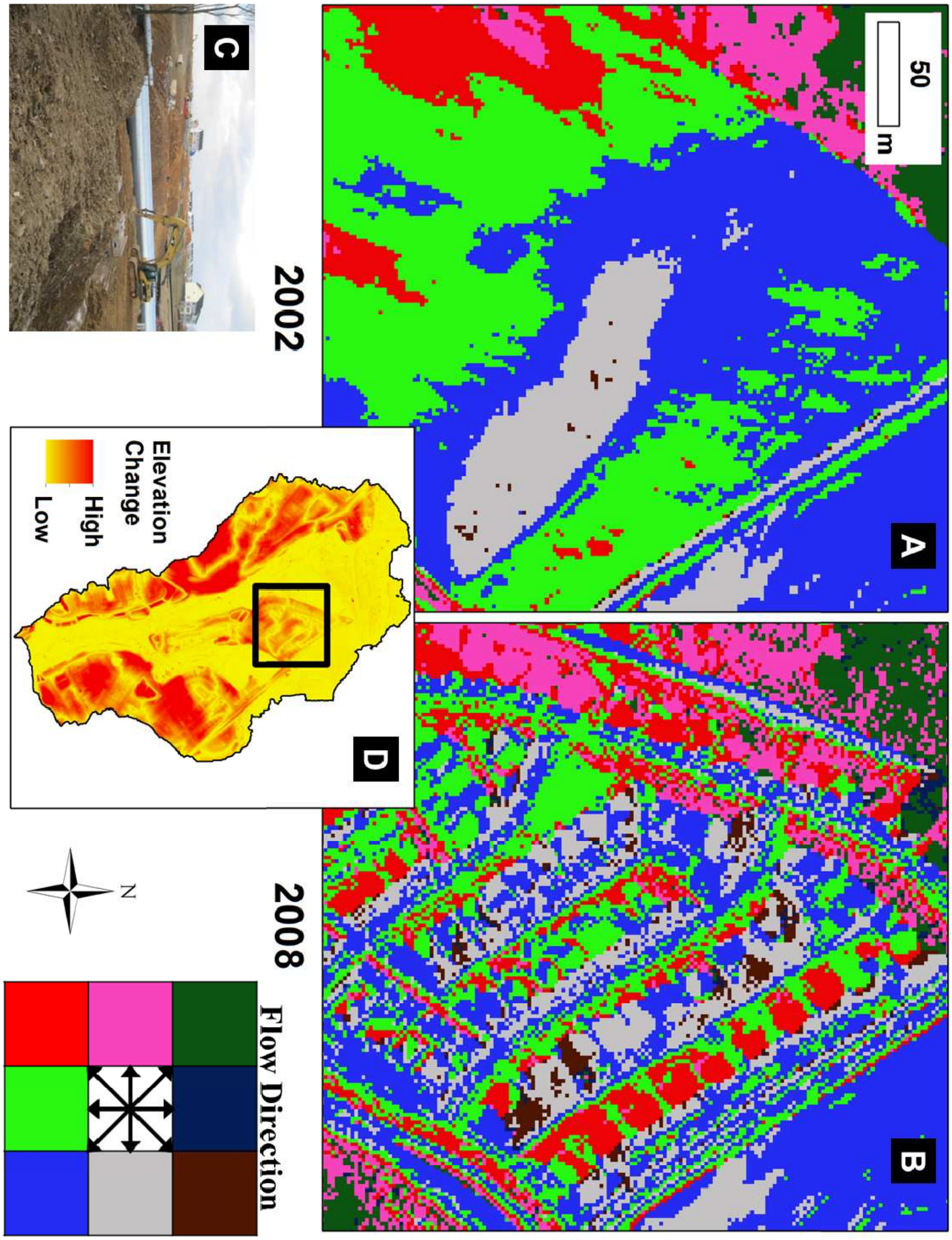
A
B
C
D
50 m
2002
2008
Elevation Change
High
Low
N
Flow Direction

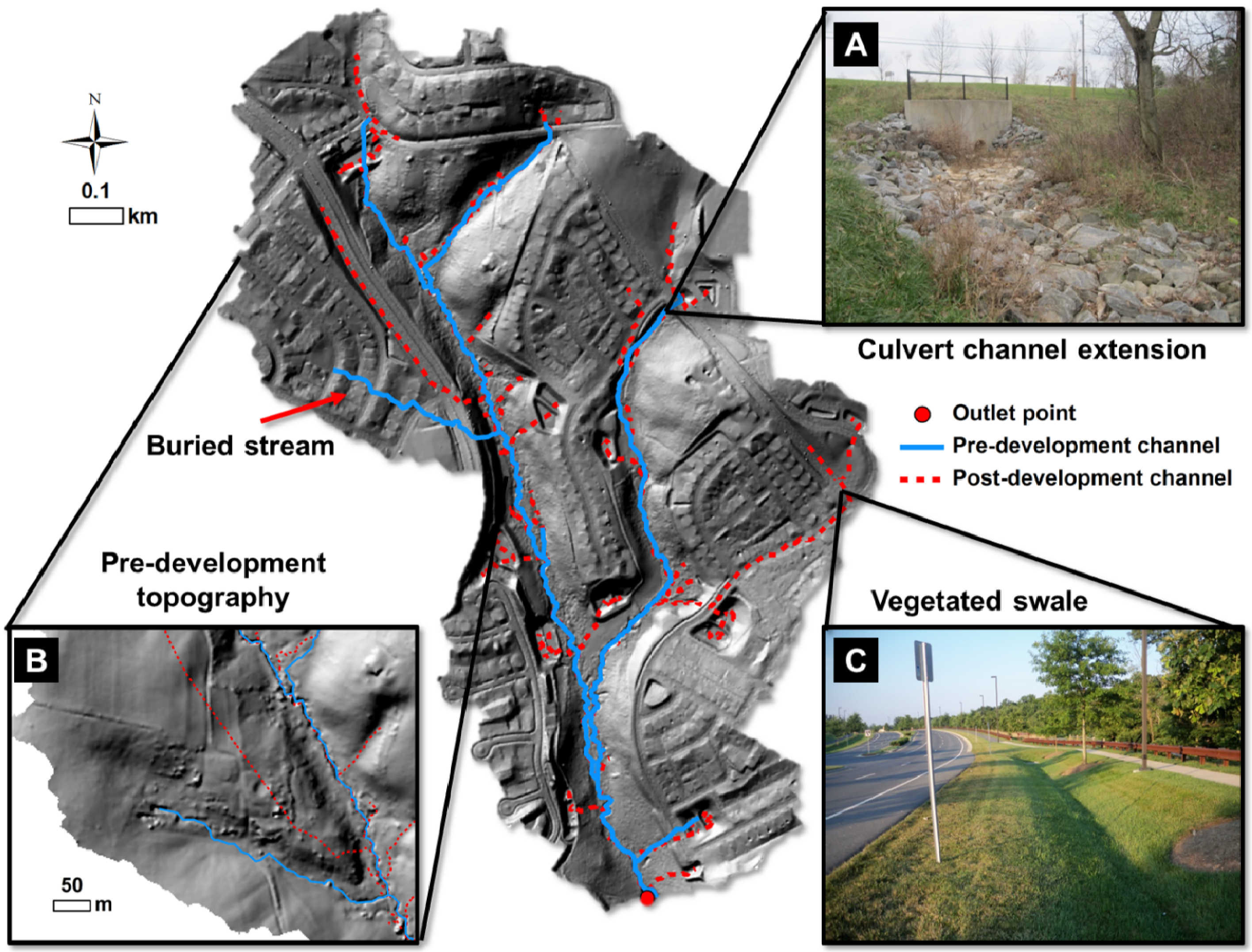
N
0.1
km
Buried stream
Pre-development
topography
B
50
m
A
Culvert channel extension
Outlet point
Pre-development channel
Post-development channel
Vegetated swale
C

Table 1

Table 1
Building removal and bare-earth point cloud processing information for each LiDAR year provided by S.T. Jarnagin (personal communication, 2013).[a]

LiDAR year	Instrument	Vendor	Building removal software	Bare-earth filtering
2002	Optech ALTM-2025	Airborne 1	Optech's REALM 2.27	Terrascan (running on Microstation)
2004	Optech ALTM-2033	Laser Mapping Specialists Inc.	Applanix POSPROC & Optech's REALM (versions not specified)	Spectra's Terramodel
2006	Optech ALTM-3100	Canaan Valley Institute	Optech's REALM (version not specified)	Microstation 8 with Terrascan
2007	Optech ALTM-3100	Canaan Valley Institute	Optech's REALM (version not specified)	Microstation 8 with Terrascan
2008	Leica ALS-50	Sanborn	Applanix POSPROC 4.3	Leica ALS post-processing and Terrasolid Terrascan

[a]Any use of trade, firm, or product names is for identification purposes only and does not imply endorsement by the U.S. Government.

Table 2

Table 2
Slope classes and associated economic costs and considerations for urban development (adapted from Csima, 2010)

Angle of slope	Development potential and the required landscaping
Up to 5%	Easy and economic development potential. In general, terracing not necessary; landscaping exclusively restricts to drainage. Relief does not pose a limit either to buildup density or building size.
5-12%	Increased development costs. Landscaping is inevitable; development is only possible with terracing and slope leveling. Somewhat limited development.
12-25%	Development potential at significant cost and labor expenditure, only with terraces and supporting walls provided. Major topographic transformation; relief fundamentally controls the type of development to be applied.
25-35%	Limited potential for urban development. Low building density with small-sized buildings.
Above 35%	Unsuitable for urban development.

Figure 1
Click here to download high resolution image

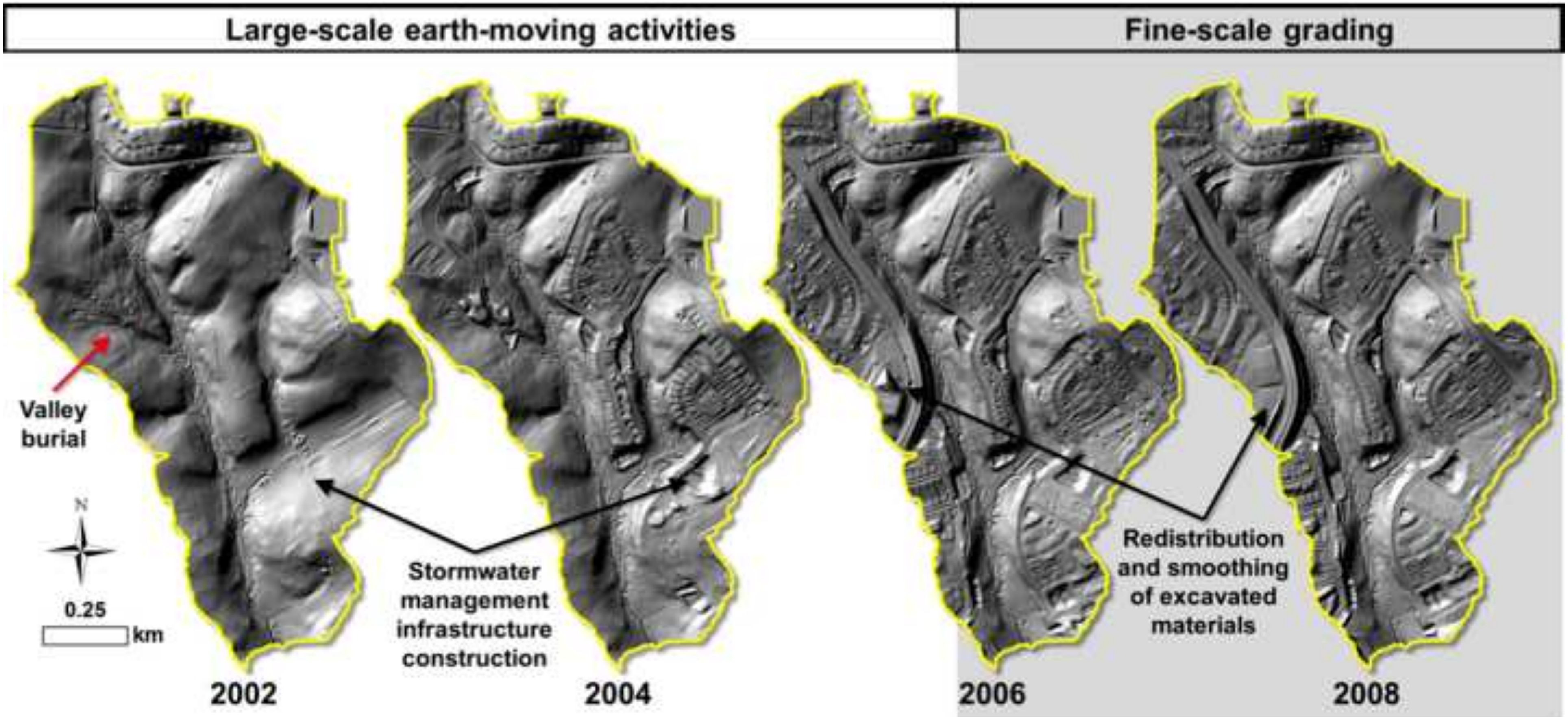

Figure 2
Click here to download high resolution image

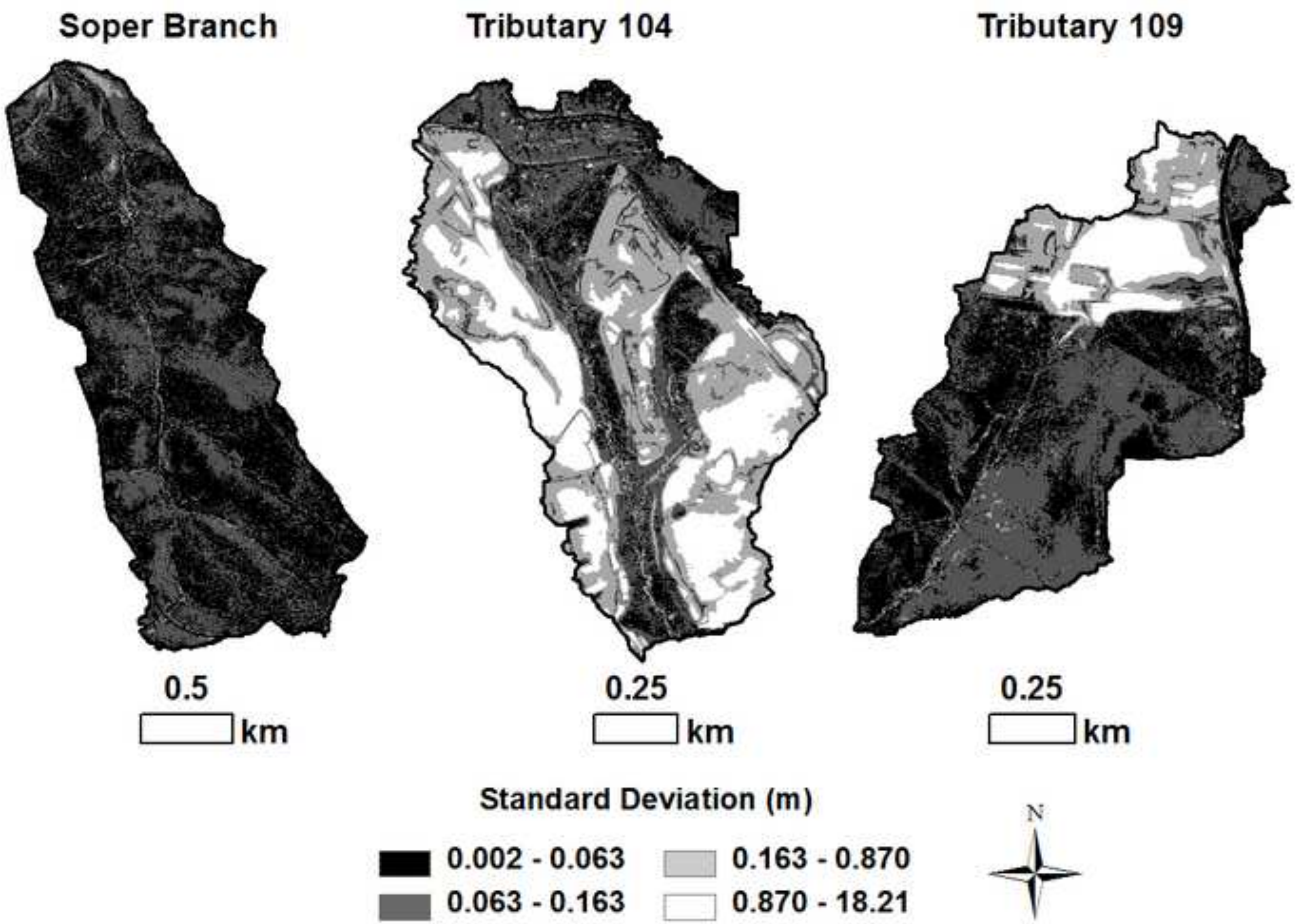

Figure 3
Click here to download high resolution image

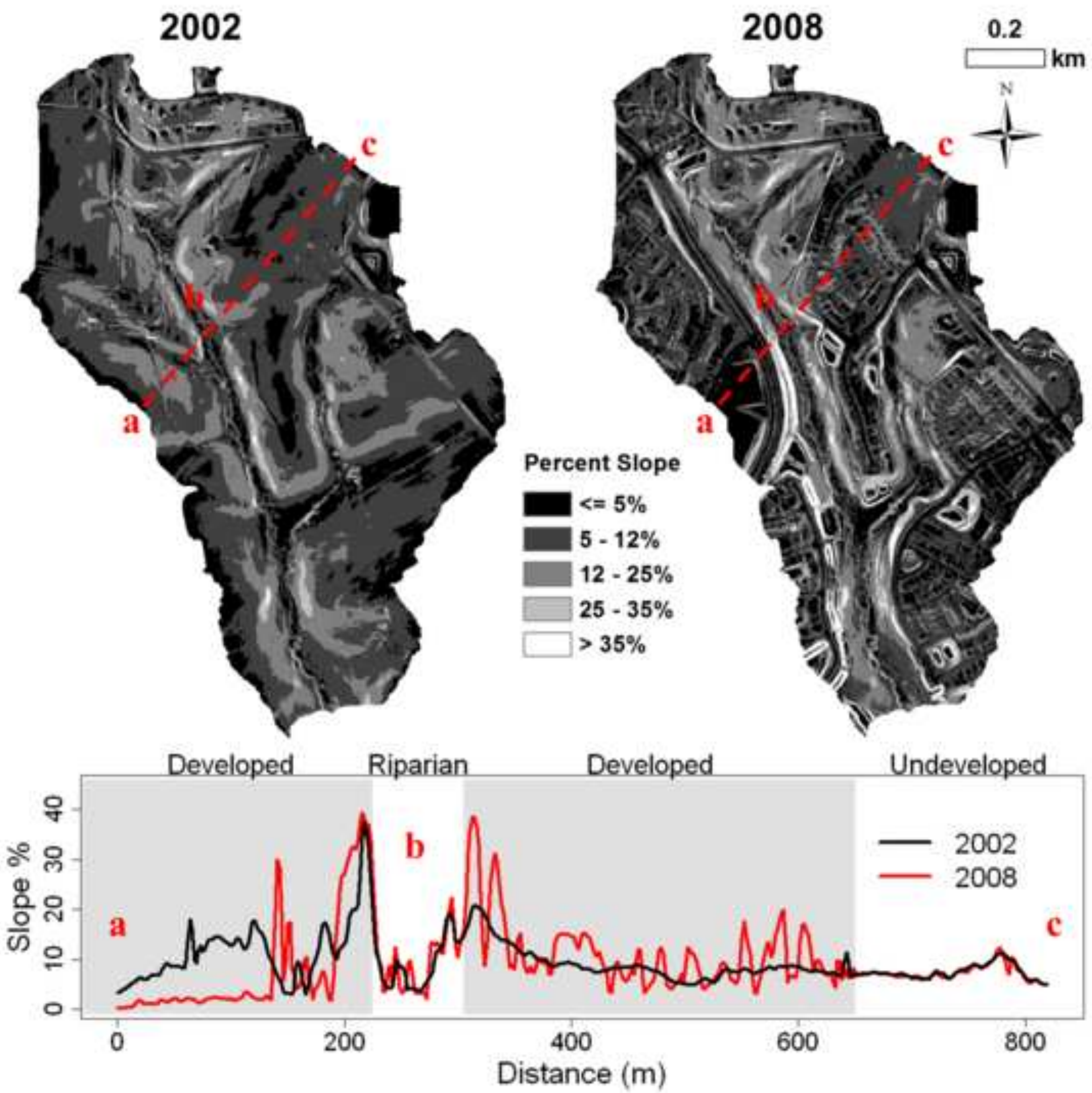

Figure 4
Click here to download high resolution image

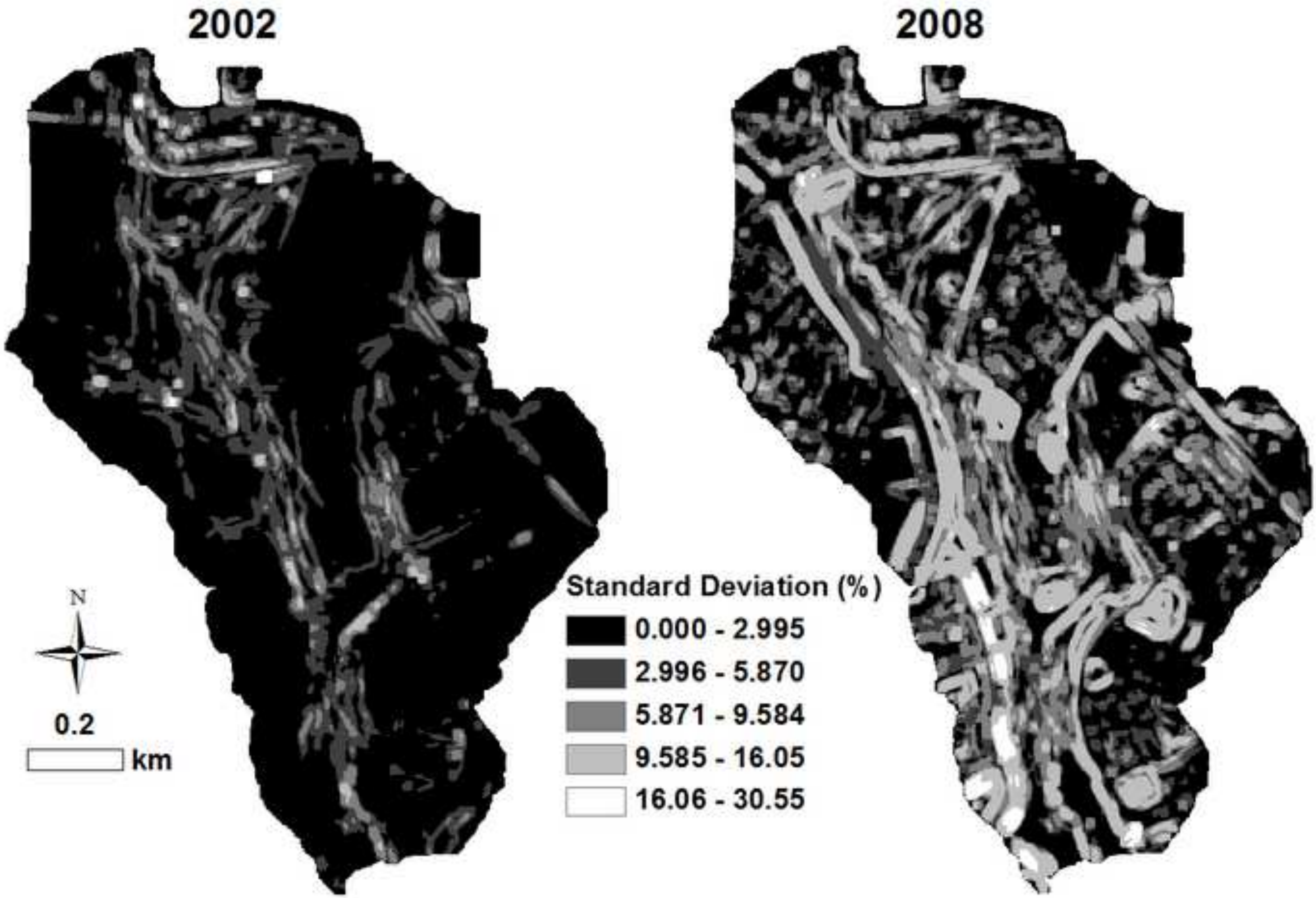

Figure 5

Click here to download high resolution image

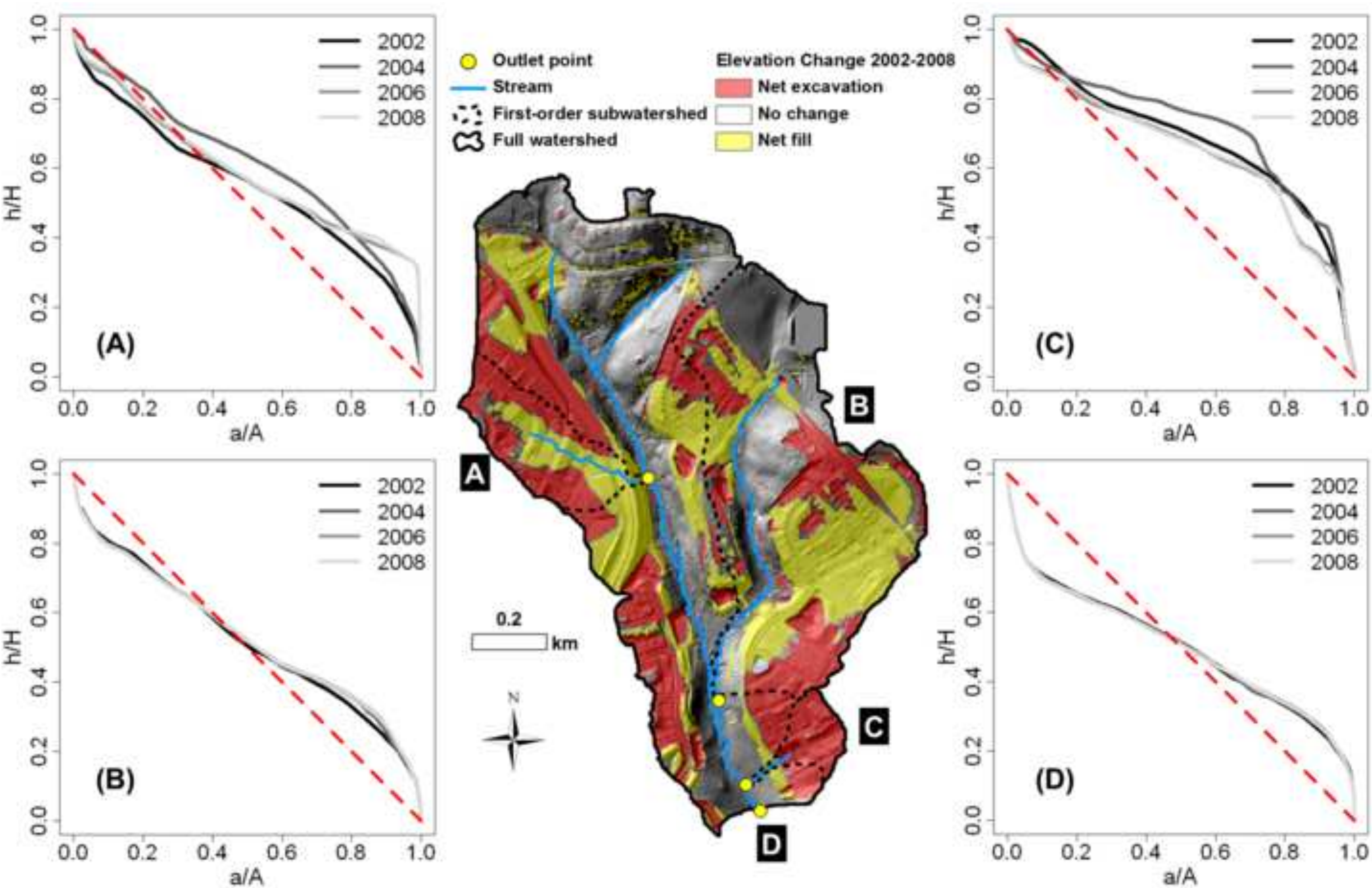

Figure 6
Click here to download high resolution image

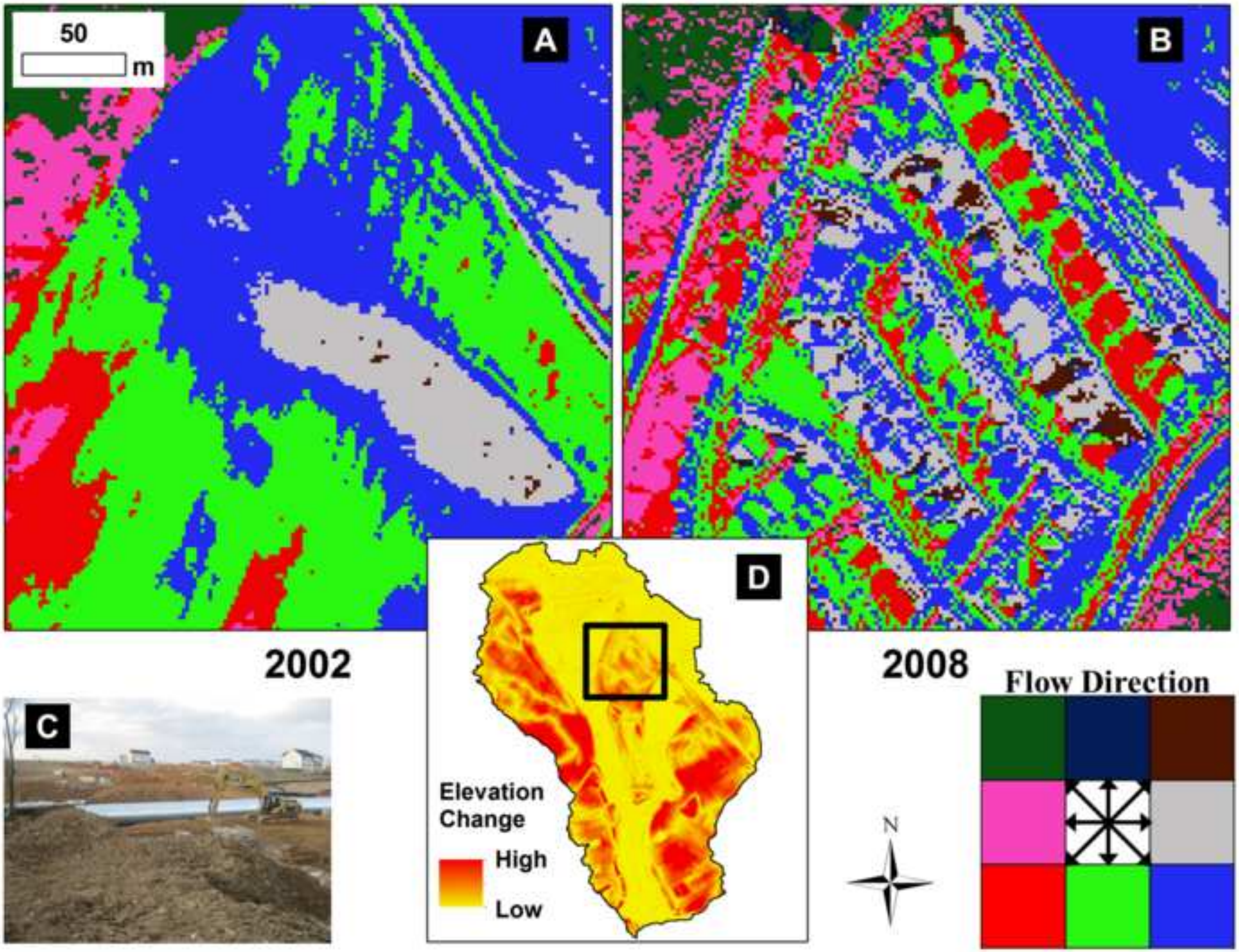

Figure 7

Click here to download high resolution image